

Lightning Detection and Warning



**Anirban Guha, Yakun Liu, Earle Williams, Carina Schumann,
and Hugh Hunt**

Abstract This chapter is concerned with the remote detection and analysis of thunderstorms and lightning flashes by electrostatic, electromagnetic and photographic means, and the use of these methods for public warning of hazardous conditions. Section 1 addresses the measurement of electrostatic fields in fair weather and in response to the stronger fields of electrified shower clouds and thunderstorms. Section 2 reviews various methods in place worldwide for the detection of the electromagnetic radiation from lightning. The observation of the evolution of lightning flashes with video-camera observations is the subject of Sect. 3. The final Sect. 4 addresses the dissemination of the multitude of available observations for purposes of improving lightning safety.

Keywords Electrostatic fields · Video-camera observations · Electromagnetic radiation · Nowcasting · Detection

A. Guha

Department of Physics, Tripura University, Agartala, Tripura, India
e-mail: anirbanguha@tripurauniv.in

Y. Liu · E. Williams (✉)

Department of Civil and Environmental Engineering, Massachusetts Institute of Technology,
Cambridge, MA, USA
e-mail: earlew@ll.mit.edu

Y. Liu

e-mail: yakunliu@mit.edu

Y. Liu

Department of Electrical Engineering, Shanghai Jiao Tong University, Shanghai, China

C. Schumann · H. Hunt

Johannesburg Lightning Research Laboratory, School of Electrical and Information Engineering,
University of the Witwatersrand, Johannesburg, South Africa
e-mail: carina.schumann@wits.ac.za

H. Hunt

e-mail: hugh.hunt@wits.ac.za

© The Centre for Science and Technology of the Non-aligned
and Other Developing Countries (NAM S&T Centre) 2021

C. Gomes (ed.), *Lightning*, Lecture Notes in Electrical Engineering 780,
https://doi.org/10.1007/978-981-16-3440-6_2

1 Measurement of Electrostatic Fields

One of the earliest quantitative devices for registration of the electrical potential gradient in fair weather conditions was Lord Kelvin's water dropper [1, 2]. Water drops are charged by induction in the electric field to be measured, and emitted from an elevated water container electrically insulated from ground, until the electric potential of the container matches that of the local potential of the atmosphere. The potential of the container is then measured with a high-impedance electrometer (also of Lord Kelvin's design [2]). The value of this potential with respect to local ground is the "potential gradient", and also explains how this terminology entered atmospheric electricity research in the early days.

Other instruments known as electric field mills are most commonly used [3] to record the large departures from fair weather potential gradient (~ 100 V/m) associated with charge separation in electrified clouds and thunderstorms. Since precipitation is almost invariably present in such circumstances, the use of the water dropper described above is not practical. A field mill consists of a set of fixed stator plates, isolated from ground, which are alternatively exposed and shielded by a motor-driven rotating, grounded conductor. The surface charge density, σ , induced on a stator plate by the applied electric field E (in volt/m) is given simply by in Eq. (1).

$$\sigma = \epsilon_0 E \text{ Coulombs/m}^2 \quad (1)$$

It is the current flow to and fro from the stator plates that constitutes the field mill "signal", and is directly proportional to the imposed electric field one wishes to measure. The sensitivity of a field mill can be increased by increasing the area of the stator plates, and by increasing the frequency with which they are alternately exposed and shielded. The time resolution of a field mill is set by this latter frequency. All field mills have capability to resolve the abrupt changes in electrostatic field accompanying both intracloud and cloud-to-ground lightning flashes, and so can be used to estimate total lightning flash rates to distances up to 10–20 km from the parent storms.

Field mills can be installed and absolutely calibrated at the Earth's surface by flush-mounting the stator plates with a large grounded metal plate mounted directly on a flat patch of earth's surface. In the typical calibration exercise, a second large metal plate can then be placed on insulator stand-offs over the operating field mill. Well defined voltage differences can then be applied (with ordinary batteries) between the covering plate and ground to replicate specific values of electric field in units of volts per meter.

To protect against short-circuiting of the stator plates in heavy rainfall, so-called inverted field mills can be installed on short grounded conductive masts, with the field mill rotors and stator plates facing downward. The conductive mast serves to distort the local electric field from uniformity, and so additional work is needed in this kind of installation for absolute calibration.

2 Electromagnetic Detection of Lightning Flashes

2.1 Introduction

Lightning discharges produced by thunderclouds can be broadly separated into two main categories, ground flashes and cloud flashes [4, 5]. Cloud flashes are roughly 5 to 10 times more numerous than ground flashes, whereas ground flashes gain more attention as they can cause severe damage to electric power transmission lines, wind turbines, oil storage tanks, etc.. Ground flashes are manifest as a direct highly ionized hot plasma with typical peak temperature reaching 30,000 K, a transient intense current and high voltage injector, and an instantaneous source of electromagnetic radiation [5, 6]. Detection of ground flashes serves to supply basic lightning data for nowcasting and forecasting in specialized applications, protection of human and industrial activity, damage recognition and verification, and for study of climate change and many other lightning-prone areas [7–9].

Ground flashes, also known as cloud-to-ground (CG) flashes, are generally grouped into four categories based on the specific pathway and its current directions within the lightning channel: (1) the downward negative ground flash, (2) upward negative ground flash, (3) downward positive ground flash, and (4) upward positive ground flash [10]. Complex transient electric discharge processes usually occur in ground flashes within hundreds of milliseconds and even a few seconds from cloud to ground. A CG lightning specifically consists of the preliminary breakdown, stepped leader, attachment process, first return stroke, K-process, J-process, dart leader, continuing currents, M-component, and subsequent strokes [10]. These individual physical processes are associated with different characteristic electric and magnetic fields corresponding to significant electromagnetic energy in the radio frequency range from below 1 Hz to ~300 MHz [11]. Although the frequency of electromagnetic radiation emitted by lightning can be up to 10^{20} Hz or more (such as X-rays), this kind of emission is usually undetectable beyond ~1 km from the source at ground level [12]. Large range (a few thousand kilometers) detection technology of ground flashes generally chooses the practically and discernibly observable electromagnetic signals to infer lightning parameters. The acoustic and optical radiation from a lightning source are limited to close detections due to their apparent attenuation with distance. In this Section, the lightning processes and electromagnetic signatures will be introduced in detail in Sect. 2.2. Principles of lightning detection are addressed in Sect. 2.3. Section 2.4 describes the early history of lightning detection and Sect. 2.5 presents some examples of modern lightning detection systems.

2.2 Lightning Processes and Electromagnetic Signatures

Most (accounting for ~90%) of CG discharges are initiated within the cloud charge structure and transfer negative charges to ground in an overall downward developing

direction, namely the downward negative lightning discharge. This kind of downward negative lightning discharge is taken as an example to briefly depict the lightning processes and its electromagnetic signature. The basic element in the CG discharge is termed the component stroke, or simply 'stroke'. A ground flash commonly contains several (typically 3–5) strokes with time intervals of tens of milliseconds [13]. These strokes terminate at different ground points spatially separated by up to a few kilometers in the 30–50% of all flashes. For video-camera documentation of the strokes of a flash, see Sect. 3.

Ground flashes are initiated by the preliminary breakdown (PB) process, often referred simply as 'initial breakdown' [14]. Preliminary breakdown occurring within the cloud usually lasts a few tens of milliseconds and tends to produce impulsive narrow radiation bursts on a microsecond scale. The PB process sets the stage for the initiation of a downward-moving stepped leader (SL). This leader is an ionized discharge channel and intermittently develops downward to ground with an average speed of $\sim 2 \times 10^5$ m/s over a time interval of a few tens of microseconds between consecutive discrete steps [15]. Each step is associated with a current pulse of 1 kA or greater and has a time duration of typically 1 μ s and each develops over tens of meters in length. The entire stepped leader process is usually transpiring within a time scale of tens of milliseconds and with an average leader current of some hundreds of amperes. New lightning channels are forged in the above breakdown stages and in the process emit a dominant electromagnetic energy in the Very High Frequency (VHF) band. During the SL process, a variation in electromagnetic radiation usually occurs from impulsive radiation bursts associated with step development to continuous radiation bursts accompanied by the leader approaching ground with complex branched structure [16].

Generally, when a stepped leader is progressing downward to ground, one or more upward-moving leaders with some tens of meters of length originate from the ground or from the tips of objects and attempt to contact the associated branches of the downward leader and generate single or multiple channel connections [17]. Successful connections represent the attachment process. The last connection stage for the extending plasma channels of downward and upward leaders is known as the break-through phase or 'final jump', indicating that the discharge channel in the air transforms from a relatively low-conductivity streamer into a high-conductivity plasma channel. Meanwhile, one downward moving return-stroke wave and another upward moving return-stroke wave are launched from the junction point and propagate along the lightning channel, thereby initiating the return stroke process. In the case of a subsequent stroke, a second attachment process may occur with an upward connecting leader length of ~ 10 m shorter to cater to the dart leader [13].

The return stroke is the most recognizable process of a ground flash in terms of both the optical brightness and the electromagnetic signature. The return stroke serves to neutralize the leader charge with a typical average speed of 1/2 to 1/3 of the light speed and is accompanied with a transient brightening of the lightning channel [18]. The peak temperature of the lightning channel rises rapidly to $\sim 30,000$ K, creating a high pressure of the order of 10 atmospheres or more and an outward propagating shock wave during the channel expansion. The peak current of the first return stroke

is typically some tens or even hundreds of kiloamperes with a risetime (from 10 to 90% of the peak current) of some microseconds and with a decay to half-peak value within several tens of microseconds. By contrast, the current in the subsequent return stroke usually shows a lower peak amplitude but shorter risetime in less than a microsecond and a droptime to its 50% value in a few tens of microseconds. The electric and magnetic field radiated by return strokes shows a conspicuous initial field peak in the recorded waveforms beyond ~10 km. The mean initial electric field ranges typically from 6–8 V m⁻¹ for the first return stroke and 3–6 V m⁻¹ for subsequent return strokes, with range-normalizing to 100 km [19]. These return strokes emit the most powerful electromagnetic radiation in low frequency (LF) and very low frequency (VLF) ranges. A representative electric field changes radiated from a CG flash (distance = ~60 km) is shown in Fig. 1 [20].

The maximum in radiated electric field for the lightning return stroke in the VLF frequency range (see Fig. 2) can be understood by considering the vertical return stroke channel as resonant antenna with length equal to a half-wavelength. For a typical vertical length of 7 km (a typical height to the main negative charge of a

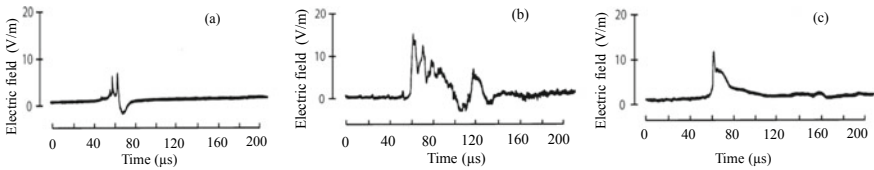


Fig. 1 Representative electric field changes radiated from a CG flash (distance = ~60 km). **a** Preliminary breakdown within the cloud. **b** First return stroke. **c** A subsequent return stroke in the preexisting channel [20]

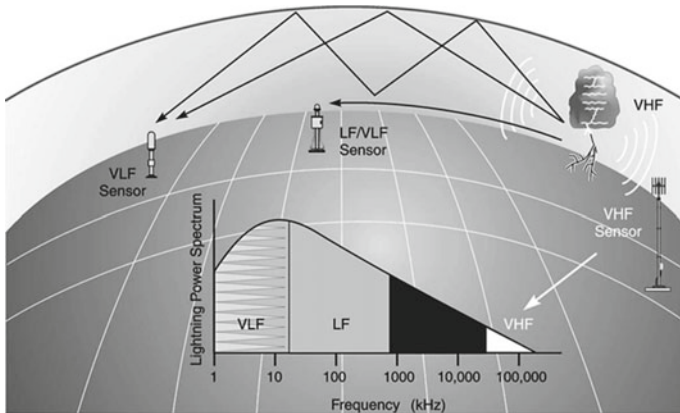


Fig. 2 Illustration of lightning locating techniques and operating frequencies. The spectral maximum lies in the upper VLF frequency range, in agreement with radiation expected from a half-wavelength resonant dipole

thunderstorm), the resonant emission has a dominant wavelength $\lambda = 14$ km and a dominant frequency f given by the dispersion relation in Eq. (2).

$$f\lambda = c \quad (2)$$

where c is the speed of light. Solving for f gives ~ 20 kHz, in the upper VLF frequency range.

Between the return stroke and the initiation of the dart leader, the J- (for junction) and K- processes occur within the cloud preceding a dart leader and transport additional charge into the existing lightning channel [21]. The J-process is characterized by a relatively steady electric field change lasting tens of milliseconds, which is generally weaker than the field change induced by a continuing current. The K-process generally produces transients and rapidly changing electric fields that are superimposed on the overall electric field associated with the J-process at time intervals of several to tens of milliseconds. The dart leader propagates downward with a speed of $\sim 10^7$ m/s and typically shows a peak current of ~ 1 kA [22]. The occurrence of the dart-stepped leader or stepped leader as a leader closing with ground depends on whether the leader progresses following the path of the preceding return stroke or not. A new termination will form when the dart or dart-stepped leader deflect from the previous return-stroke path. The radiation from a dart leader is generally continuous with variable amplitude and occasionally accompanied with some pulses [16].

The continuing current process often follows subsequent return strokes and maintains a current magnitude of tens to hundreds of amperes for up to hundreds of milliseconds. 30~50% of the negative ground flashes contain continuing currents with durations in excess of 40 ms, often defined as the long continuing current [23]. The lightning channel during the continuing current process exhibits a relatively faint luminosity and usually exhibits intermittent luminous surges superimposed on that faint luminosity. These surges are called M-components, with a peak current of typically hundreds of amperes and a risetime in the range 300~500 μ s. The electric field changes associated with M-components recorded at a close range (mostly 6 km or less) exhibit a characteristic hook-like shape with a typical duration less than a few microseconds [24]. For information on the video-camera detection of lightning M-components, see Sect. 3. A representative E-field of the K-change, J-change, leader and return-stroke, and M-component in a flash adapted from Thottappillil et al. [25] is shown in Fig. 3.

2.3 Principles of Lightning Detection

Lightning information has wide and important applications and is expected to be monitored in all corners of the world. A large number of ground-based and space-based lightning detection sensors or systems have been invented to locate lightning

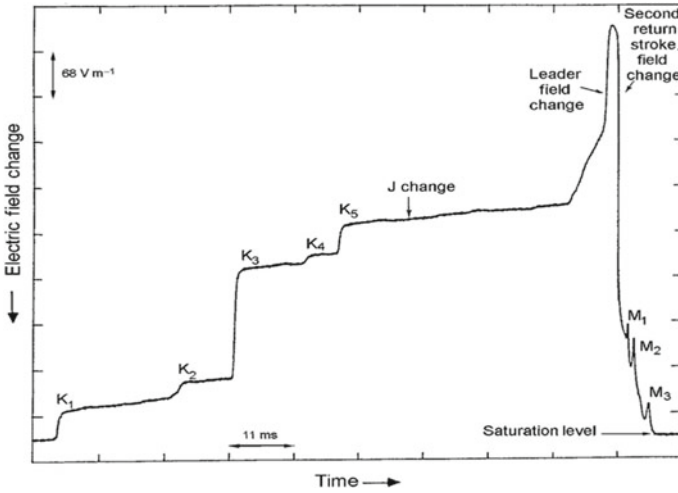


Fig. 3 Partial electric field change of a flash at a distance of 2.5 km (Florida 2228:43 UT 1979). K_1 – K_5 are five K-changes. The J-change, leader and return-stroke E-field change are presented. M_1 – M_3 are E-field changes of three M-components [25]

and measure its parameters. Space-based lightning detection sensors mainly monitor total lightning (ICs and CGs) by capturing the optical transient from lightning. The detection sensor is conceptually a high speed event detector onboard an Earth orbiting satellite, which typically consists of a real-time event processor, a high speed Charge Coupled Device (CCD) focal plane, a wide field-of-view lens, and a narrow-band interference filter [26]. It has a wide detection coverage but with a relatively-low spatial resolution (~ 1 km or less) and is generally incapable of distinguishing ICs and CGs, limiting itself primarily to meteorological service. Space-based sensors can also monitor the electromagnetic emissions (VHF) and detect lightning over large regions [27–29], such as the lightning-associated VHF signal measured by the Fast On-Orbit Rapid Recording of Transient Events (FORTE) satellite [30, 31]. There is no publicly available VHF-based multi-satellite lightning geolocation system.

Ground-based lightning detection sensors monitor electromagnetic radiation in different frequency ranges with selection based on multiple factors. Due to the complexity in the wide-ranging amplitudes and waveforms associated with lightning, it is difficult to accurately locate an individual lightning flash with a single ground-based sensor. Lightning detection geographical coverage and spatial resolution depend on the total number of sensors and the selected frequency. The monitoring of radiation in the VHF range (30–300 MHz) will allow a lightning detection system with a resolution of 1–10 m but will require more sensors more closely deployed because of geometrical attenuation and the absence of over-the-horizon propagation. If a lightning detection system uses the LF (30–300 kHz) or VLF (3–30 kHz) range, the natural global waveguide can be exploited and the lightning detection coverage area can be enlarged efficiently with a more modest numbers of sensors, but with

substantial sacrifice of spatial resolution on individual lightning flashes. Uncertainties of order 1 km or more for the LF approach and in the 10 km range for VLF signals can be anticipated.

Three kinds of multi-station locating techniques are commonly used for detecting the electromagnetic emissions from lightning: (1) magnetic direction finding (MDF), (2) time of arrival (TOA), and (3) interferometry, which are each detailed in the following discussion.

The magnetic direction finding (MDF) approach utilizes two horizontal orthogonal loops with directions oriented East–West (EW) and North–South (NS) to detect the magnetic field emitted from a CG flash, a quasi-vertical electromagnetic radiator from cloud to ground discussed earlier. Based on Faraday’s law of induction, the acquired voltage of a given loop is proportional to the rate of change of the magnetic flux through a region of space enclosed by the loop. Hence, the tangent of the angle between north and the CG flash location as viewed from the sensor is linearly related to the induced voltage ratio of the NS/EW loops. Two types of crossed-loop magnetic direction finders are commonly used in lightning detection, the narrow band (tuned) and the gated wideband magnetic direction finders. The general frequency employed in narrow band magnetic direction finders ranges from 5–10 kHz to capture the peak frequency spectrum for lightning. The attenuation is relatively low in the Earth-ionosphere waveguide. The narrow band magnetic direction finder has a long application history beginning in the 1920s but it has inherent azimuthal errors (also named polarization errors, or site error corrections) on the order of 10° in close ($< \sim 200$ km) lightning detection due to an undesired voltage induced from the non-vertical lightning channel segments and also due to the inhomogeneous conductivity of the ground beneath the station. The gated wideband magnetic direction finder was developed in the 1970s to overcome this shortcoming by adding a gate on the sampling of magnetic field, focusing the analysis on the initial peak from the return stroke. This initial peak contains radiation from the lowest hundreds of meters of the lightning channel, where it tends to be straight and vertical. The gated wideband magnetic direction finder usually operates in the frequency range of a few kHz to 500 kHz and excludes the ionospheric reflections. Magnetic direction finders are susceptible to the unwanted magnetic field from the surroundings. Therefore, it is recommended to select a flat and uniform area, as well as one without conducting structures or buried objects, so as to reduce the site errors.

The time of arrival (TOA) technique locates lightning on the basis of the arrival times of electromagnetic signals at the detection sensors. These sensors usually operate in different frequency ranges of VHF (30–300 MHz), LF (30–300 kHz), and VLF (3–30 kHz), and can be generally divided into three types, (1) very short baseline (tens to hundreds of meters), and (2) short baseline (tens of kilometers) operated at VHF, and (3) long baseline (hundreds to thousands of kilometers) operated at LF and VLF. A very short baseline TOA system consists of two or more TOA receivers and locates lightning from the intersection of hyperboloids deduced from the arrival time differences of every individual VHF pulse. It is capable of resolving air breakdown processes with a time accuracy of tens of nanoseconds. A short baseline TOA system typically uses 5–15 stations as a network to map lightning channels

in three-dimension. This system can depict the temporal and spatial development of lightning charges, which has become a major tool for lightning research and operational applications. A long baseline TOA system operates at LF/VLF and generally needs four or more stations to assure a unique lightning location as the hyperbolae from two arrival time differences intersect at two points on the Earth's surface for a remote lightning. The detection system is most sensitive to the return stroke and has a wide coverage of lightning detection of hundreds to thousands of kilometers.

The interferometry technique detects the phase difference between narrow band signals associated with the noise-like bursts produced from lightning by using two or more closely spaced (usually several meters distance) sensors. There is no requirement to identify an individual pulse in this approach. A lightning interferometer is usually composed by two or more identical antennas separated by a few meters and connected by the same narrow-band filter and receiver. The phase difference between two quasi-sinusoidal signals out of the two receivers is then converted into a voltage by a phase detector. Three or more antennas are necessary to form two or more orthogonal baselines in order to obtain the azimuth and elevation of a radiation source. Interferometric systems usually operate in very narrow frequency bands within the VHF band (30~300 MHz)/UHF (ultra-high frequency, 300 MHz–3 GHz) and consist of two or more synchronized interferometers separated by some tens of kilometers or more to locate lightning in three dimensions. These systems have high sensitivity to the signal but also with relatively low signal-to-noise ratio due to the high working frequency and antenna spacing limitation. In the installation of the antenna array, the surrounding obstacles and other noise sources should be cleared to eliminate perturbations and coupling between antennas.

2.4 Early History of Lightning Detection

Lightning has been studied for hundreds of years. In June 1752, Benjamin Franklin performed the famous Kite experiment in Philadelphia and identified lightning as an electrical discharge [32]. In 1895, Popoff used a coherer (a primitive form of radio signal detector) and made the first measurement with purpose to investigate the electromagnetic fields emitted by lightning [33]. The duration of lightning was estimated by De Blois with using an ordinary wireless aerial of feeble damping together with an oscillograph (of natural periodicity 5000–6000) and a rotating mirror [34]. With the advent of the cathode-ray oscilloscope, Watson-Watt and Appleton succeeded in recording the radiation field waveforms visually during 1922–1923 and firstly analyzed the atmospheric radio signals quantitatively [35]. In the development of radio communication, the electromagnetic radiations produced by lightning were generally measured by the narrow-band radio receivers or antennas in the LF and VLF ranges with a motivation to solve the interference problem in long-range radio communication from lightning flashes (the 'sferics') [36].

During World War II, the narrow band VLF lightning detection system was utilized and consisted mainly of two or more magnetic direction finders with a lightning

location accuracy of tens of kilometers. The gated wideband magnetic direction finder was developed in the 1970s to overcome this shortcoming of polarization errors in the narrow band magnetic direction finder. The time-of-arrival technique was developed in the 1930s, driven by the demands for marine navigation, and was introduced into lightning location methods in the late 1950s. Oetzel and Pierce first suggested the very short baseline TOA technique to be employed for line-of-sight location of lightning VHF sources in 1969. Three years later, [37] used one pair of antennas with operating frequency in the range 25–35 MHz and successfully verified the TOA direction finding technique. Two short-baseline VHF TOA systems have seen extensive use since the early 1970s, the 253 and 355 MHz systems developed in South Africa and the Lightning Detection and Ranging (LDAR) system (central frequency between 56 and 75 MHz) developed at the NASA Kennedy Space Center [38]. The first long-baseline TOA system, implemented by a pair of receiving stations separated by over 100 km in Massachusetts and operated at VLF and LF (bandwidth of 4–45 kHz), enabled Lewis et al. (1960) to compare time arrival differences for the two stations. Warwick et al. (1979) first designed an interferometer to detect lightning. An improved version of the interferometric system was later developed by the research group at the New Mexico Institute of Mining and Technology [39, 40].

More detailed description on the early history of lightning detection can be found in Uman and Rakov [13] and Cummins and Murphy [36]. The following subsection 2.5 will introduce some modern lightning detection systems together with their respective detection technique and operating frequency.

2.5 Examples of Modern Lightning Detection Systems

Substantial demand from the long-standing scientific interest and practical application has motivated the advancement of lightning detection systems. The lightning locating techniques and operating frequencies are illustrated in Fig. 2. The Lightning Mapping Array (LMA) developed by New Mexico Institute of Mining and Technology will be first introduced as it can give the most complete record of the spatial and temporal development of lightning channels. The typical LMA is also equally sensitive to both intracloud and cloud-to-ground lightning detection, and so stands apart from many of the other detection systems that will be described afterward. The globally-oriented Earth Networks Total Lightning Network is also designed for intracloud lightning detection. Many countries have developed their own lightning detection systems, such as the U.S. National Lightning Detection Network (NLDN), the Canadian Lightning Detection Network (CLDN), the Brazilian Lightning Detection Network (BrasilDAT), the Lightning detection NETWORK (LINET) and the European lightning location system EUCLID, the Italian LAMPINET (LAMPI for ‘flash’ in Italian, NET for network), the Spanish Lightning Detection Network (SLDN) and the Catalan Lightning Detection Network (XDDE), the lightning detection networks in

China, and the South African Lightning Detection Network (SALDN). Three additional lightning detection systems are aimed at the measurement of the global lightning, the World Wide Lightning Location Network (WWLLN), the Global Lightning Dataset (GLD360), and the Earth Networks Total Lightning Network (ENTLN). All these modern lightning detection systems will be briefly reviewed. In addition, single lightning flashes of mesoscale extent (>100 km) can singlehandedly excite the global Schumann resonance intensities 10–100 times the level of the “background” lightning activity, which can be located globally from a single receiving station equipped with sensors for vertical electric field and horizontal magnetic field. The geo-location method and characterization of these ELF transients is also introduced in brief.

(1) Lightning Mapping Array (LMA)

The deployable Lightning Mapping Array (LMA) was developed on the basis of the Lightning Detection and Ranging (LDAR) system used at the NASA Kennedy Space Center [38, 41]. The system uses six or more stations with time synchronized by GPS technology to independently measure the arrival time of impulsive VHF radiation (from both IC and CG flashes) and locate lightning by the VHF TOA technique [42]. Measurement stations are usually deployed over an area typically 60 km in diameter with each station separated by 15–20 km and connected via wireless communication links to a central site for processing. Each station monitors the peak intensity of VHF radiation in a 6 MHz bandwidth centered at 63 MHz (an unused television channel (channel 3)). VHF radiation (time and magnitude) is recorded in every 80–100 μ s time interval. The peak signal times are measured with a high-time resolution (~ 50 ns) by a digitizer accurately phase locked to the 1 pulse-per-second output of a GPS receiver [43, 44].

The LMA has provided unprecedented details on the temporal and spatial evolution of lightning discharges by locating thousands of VHF sources per flash in three-dimensional space. Thomas et al. [44] has experimentally and theoretically investigated the location accuracy of the New Mexico Tech Lightning Mapping Array (LMA) by using balloon sounding measurements, airplane tracks, and observations of distant storms. They found that sources over the network are located with an uncertainty of 6–12 m rms in the horizontal and 20–30 m rms in the vertical. The resultant 3D location errors are less than 100 m for most VHF sources and the location uncertainties for sources outside the network increase with distance [44]. The LMA system is a powerful tool to study lightning and has now been installed in other countries, such as the Brazil, Canada, China, France, Japan, United States, Spain, and others.

(2) U.S. National Lightning Detection Network (NLDN)

The U.S. NLDN has been monitoring lightning in real-time since the early 1980s and has provided continental scale (U.S.) information since 1989 [45, 46]. Its origins lie in the gated wideband Magnetic Direction Finding (MDF, commercialized by Lightning Location and Protection, LLP in the late 1970s) and currently employs

the combined TOA and MDF location methods with operating frequency range of 400 Hz–400 kHz. This system is known as the Improved Accuracy through Combined Technology (IMPACT) [36]. The U.S. NLDN now consists of more than 100 stations typically separated by less than 350 km and fully covers the contiguous United States. Both IC and CG lightning discharges can be separately identified and the peak return stroke currents are estimated from the measured fields. The detection efficiencies and location accuracy of the CG stroke and flash have been investigated by using GPS-synchronized video cameras in conjunction with broadband electric field and optical (light pulse) recordings in Southern Arizona, Oklahoma, and Texas [47], in the Central Great Plains [48], and by the ground-truth rocket-triggered lightning at the International Center for Lightning Research and Testing (ICLRT) in Florida [49, 50]. The stroke detection efficiency is estimated to be 76% ($N = 3620$) in Arizona, 85% ($N = 885$) in Texas/Oklahoma, 84% ($N = 547$) in the Central Great Plains, and 76% ($N = 139$) at ICLRT. And the corresponding flash detection efficiencies are 93% ($N = 1097$), 92% ($N = 367$), 91% ($N = 342$), and 92% ($N = 37$), respectively. More information about the NLDN, such as the evolution of the NLDN, its enabling methodology, and applications of NLDN data, can be found in Rakov and Uman ([13], Ch. 17), Orville [45], Orville and Huffines [46], Orville et al. [51, 52], Cummins and Murphy [36], Holle [53], and references therein.

(3) Canadian Lightning Detection Network (CLDN)

The Canadian Lightning Detection Network (CLDN), designed in 1997 and managed by Environment Canada since 1998, consists of more than 80 sensors (mainly Vaisala sensors including IMPACT- ES, LPATS-IV, LS7000, LS7001, and LS7002) and detects lightning over most of Canada to approximately 65° N in the far west, 55° N in the far east, and offshore to about 300 km [54, 55]. CLDN sensors utilize both VLF and the LF band to detect cloud-to-ground lightning and a small percentage of cloud-to-cloud lightning. CLDN determines the occurrence time, intensity, and polarity of lightning from electromagnetic (EM) pulses that lightning produces. The EM pulse information measured from each sensor is sent to the network control center in Tucson, Arizona, together with the sensor information to determine the location and other parameters of lightning [56]. The lightning information is transmitted to various clients and Environment Canada's Storm Prediction Centers. The cloud-to-ground flash detection efficiency of the CLDN is better than 90% and less than 500 m in location accuracy for a peak current threshold of 5 kA over its region of coverage [55, 56]. The CLDN and NLDN comprise the North American Lightning Detection Network (NALDN). More detailed information about the CLDN and its evaluation can be found in Burrows et al. [55], Dockendorff and Spring [56], Abreu et al. [54], Shostak et al. [57], Kazazi et al. [58], and references therein.

(4) Brazilian Lightning Detection Network (BrasilDAT)

The first systematic observations of CG lightning in Brazil were enacted in the 1960s based on the number of thunderstorm days at different sites [59]. The first lightning location system in southeast Brazil was a small regional network installed in 1988 and consisted of four Lightning Positioning and Tracking System (LPATS) sensors using

the TOA technology [60, 61]. It was later upgraded to include IMPACT sensors in 1996 and named the Brazilian Integrated Lightning Detection Network (RINDAT). In 1999, another lightning location system was installed in northern Brazil to provide ground truth data for the Lightning Imaging Sensor (LIS) in space [59]. BrasilDAT is the integrated result of two main lightning location systems and other regional networks. It has 47 stations at present including LPATS and IMPACT sensors [59]. The CG stroke detection efficiency is investigated by rocket-triggered lightning in the Southeast region of Brazil and with high-speed video camera observations. The detection efficiency is estimated to be about 55% for strokes and 87% for flashes [59, 62]. Additional information about BrasilDAT can be found in Pinto [61, 63] Pinto et al. [64–66] and references therein.

(5) Lightning Detection NETWORK (LINET)

The LINET was developed at the University of Munich beginning in 1994 and operates in the VLF/LF range [67, 68]. It has steadily expanded and now consists of more than 130 sensors (as of March 2014) across 17 countries, covering an area extending from 10°W to 35°E in longitude to 30°N to 65°N in latitude [69]. The LINET receiving station is a simple 4-part modular construction designed for easy-to-handle and economical-to-manufacture or update. Two crossed loops (without any active electronics) make up Module 1 to provide passive sensors for measuring magnetic field components in the frequency range of 1 to 200 kHz. Module 2 supplies the timing signal by using a GPS clock with an accuracy of <100 ns. Module 3 is a single plug-in device consisting of the signal amplifier, filter, and A-to-D-converter. Module 4 is a separately positioned processing unit. The incoming signal is sampled at a rate of 1 MHz and recorded with 14-bit resolution in a continuous mode. The pre-trigger time is 100 μ s and standard time window length is 512 μ s to enable inspection for occurrence of one pulse. A fast Fourier analysis and time coincidence considerations among sensors are performed to discriminate signals and eliminate noise. IC-CG classification is achieved by a specially adopted 3D-algorithm based on height (instead of the waveform differences) in the central processing unit, but the waveforms and other data are stored locally [70]. Each sensor collects data and transmits packets of condensed information to the central station at Munich. Real-time lightning location can be performed. The statistical average lightning location accuracy is ~150 m verified by strikes to towers. More details about LINET can be found in Betz et al. [6, 67, 68].

(6) European Lightning Location System (EUCLID)

The European lightning location system EUCLID was initiated by several countries (Austria, France, Germany, Italy, Norway, and Slovenia) in 2001 and then expanded to the European-wide region (Schulz et al. 2016a). The EUCLID network is now a consortium of 19 national lightning detection networks and in 2014 has 149 sensors manufactured by Vaisala Inc., 7 LPATS, 10 IMPACT, 31 IMPACT ES/ESP and 101 LS700x sensors, and operated in the same frequency range with individually calibrated sensor gains and sensitivities. The data are processed locally by each national lightning location system (LLS) [71, 72]. Additionally, the total data from all 149

sensors are handled by a central processor in Austria at ALDIS (Austrian Lightning Detection and Information System) in real-time. A full backup EUCLID processing center is set in Germany with independent and direct data connections to all sensors. Based on the ground truth data from direct lightning current measurements at the Gaisberg Tower (GBT), the detection efficiency is 96% (93% for validation by Sântis Tower, [73] and 70% for negative flashes and strokes. The median location accuracy is 89 m for the 100 strokes recorded at the GBT. The detection efficiency is 98% for negative flashes and 84% for strokes based on video and E-field recordings [74]. More details about EUCLID can be found in Pohjola and Mäkelä [75], Schulz et al. [72], Azadifar et al. [71], and Poleman et al. [76].

(7) Lightning Detection Network in Italy (LAMPINET)

The Italian Air Force Meteorological Service built the Italian lightning detection network-LAMPINET and started operation during 2004 [79] for the comprehensive detection of atmospheric discharges. LAMPINET consists of 15 IMPACT ESP³ sensors quasi-uniformly distributed over Italy and utilizes both MDF and TOA techniques [77]. The sensors monitor lightning electromagnetic field signatures and waveforms with a frequency bandwidth 1–350 kHz by means of a parallel plate capacitor for the electric field and crossed loops for the magnetic field. A GPS clock, signal analyzer, and electronics for telecommunications link each sensor to the central processing server located in the national weather center of the Italian Air Force Meteorological Service (Centro Nazionale di Meteorologia e Climatologia, C.N.M.C.A.). CG and IC classification are based on waveform criteria. C.N.M.C.A. periodically conducts data comparisons with other systems that share the same operational area with LAMPINET [78]. The LAMPINET has a detection efficiency of 90% for normalized currents higher than 50 kA and a location accuracy of 500 m in the central areas of Italy (claimed by the sensor manufacturer [78]). Larger errors are evident in the border areas of Italy and beyond the network. More detailed information about LAMPINET can be found in Biron [77], Biron et al. [78, 79].

(8) Spanish Lightning Detection Network (SLDN) and Catalan Lightning Detection Network (XDDE)

The first lightning measurement in Spain appeared in about 1904 and a keraunograph was installed at the Observatori de l'Ebre [80]. In 1992, the modern Spanish Lightning Detection Network (SLDN) was built, consisting of 14 sensors and making use of joint MDF and TOA techniques in the LF radio frequency range (similar to NLDN sensors) [81]. Now the SLND has more than 30 sensors with several expansions and covers the Iberian Peninsula, Canary Islands, and Balearic Islands [82]. The Catalan Lightning Detection Network (XDDE) was set up to detect both IC and CG discharges with 2-D location of VHF sources and initially consisted of three VHF interferometers (108–116 MHz) and covered the area of Catalonia in North-east Spain. The experimental evaluation of the XDDE was carried out with two field measurement campaigns by means of electrostatic and electromagnetic field measurements, and digital video recordings. Its CG flash detection efficiency was found to lie between 86 and 92%. The XDDE can supply valuable data to evaluate

the detection efficiency, stroke discrimination and location accuracy of the SLDN [83]. More detailed information about the SLDN and XDDE can be found in Pineda et al. [81, 84].

(9) Lighting Detection Network in China (BLNet and GHMLLS)

There are several 3D positioning systems for lightning radiation pulses (based on the TOA or interferometry techniques) and long baseline lightning location networks operating in China. The first 3D VHF lightning radiation source mapping technique installed in China operates at 270 MHz with a 3-dB bandwidth of 6 MHz and processes peak events in a consecutive time window of 50 μ s [85, 86]. A broadband electric field location system is synchronously running with an operational bandwidth from 1.5 kHz to 10 MHz. This system has a horizontal error of 12–48 m and a vertical uncertainty of 20–78 m for radiation sources validated by a balloon-borne VHF transmitter [87]. A multiband 3D lightning location network installed in Beijing, the Beijing Lighting Network (BLNet), is deployed with one data center and sixteen substations utilizing the fast antenna, slow antenna, magnetic antenna, and VHF antenna to cover a wide bandwidth from VLF to VHF [88]. The average detection efficiency of the BLNet is 93.2% for total flashes. The location error in the horizontal direction is 52–250 m based on lightning flashes to tall towers [89]. Another lightning location network in Chongqing Province is composed of 14 lightning sensors to detect VLF/LF and VHF sources radiated by lightning, and was introduced in Liu et al. [90]. The performance of lightning location systems in Guangdong Province can be found in Chen et al. [91]. The information of the Guangdong-Hong Kong-Macao Lightning Location System (GHMLLS) is detailed in Zhang et al. [92]. Additionally, two lightning observatories of the Guangdong Comprehensive Observing Experiment on Lightning Discharge (GCOELD) and the Tall-Object Lightning Observatory in Guangzhou (TOLOG) contribute comprehensive observational data to understand lightning physical processes [92–94]. More detailed information about the lightning location system and lightning observatory in China can be found in Qie et al. [95], Shi et al. [96] and Zhang et al. [92].

(10) South African Lightning Detection Network (SALDN)

The South African Lightning Detection Network (SALDN) consists of 24 Vaisala LS7000 sensors [97]. The network was originally installed in 2005 and consisted of 19 sensors. In late 2009-early 2010, three more sensors were added. A second upgrade was performed in mid-year 2011 in which two more sensors were added to the network and three of them relocated for better coverage [98]. A new flash density map was created utilizing data from the SALDN from 2006–2011 [97]. Here, ground-flash densities of 15–20 flashes/km²/year were found, indicating that the previous map was underestimating the lightning incidence in the country. The network has been evaluated against photographs of tall tower lightning events and high-speed video lightning observations. These studies show that the detection efficiency of the network has greatly improved with the addition of sensors and detects 92% of the observed downward flashes in Johannesburg, South Africa with a median location accuracy of less than 100 m [99–101].

(11) World Wide Lightning Location Network (WWLLN)

R. Dowden and is now operated by the University of Washington. This network now consists of more than 70 sensors around the globe (maintained by different participating institutions). This system utilizes a time-of-group-arrival (TOGA) method based on the fact that lightning VLF signals propagating in the Earth-ionosphere waveguide experience dispersion, in that the higher-frequency components arrive earlier than the lower-frequency components. The sensors operate in the VLF range (3–30 kHz) and measure the waveforms from sferics to calculate the TOGA [102]. Each lightning stroke location requires the TOGA from at least five WWLLN sensors. The timing accuracy is 100 ns, maintained by GPS receivers, and the uncertainty in the stroke timing is less than or equal to 30 μ s. Lightning location are characterized by an accuracy of about 5 km [103, 104]. WWLLN can detect the majority of all lightning-producing storms, even in regions with inter-station distances larger than 2000 km [105, 106]. The NLDN data have been used as the ground truth to investigate the CG flash detection efficiency of the WWLLN. The DE has increased from ~3.88% in 2006–2007 to 10.3% in 2008–2009, as the number of sensors increased from 28 in 2006 to 38 in 2009 [103]. For events with NLDN-reported peak currents ≥ 130 kA, the detection efficiency is 35% [107, 108]. Recent research indicates a detection efficiency for strokes with peak current greater than 30 kA is approximately 30% globally. More detailed information about the WWLLN can be found in <http://wwlln.net> and in Lay et al. [109].

(12) Global Lightning Dataset (GLD360)

The Global Lightning Dataset (GLD360) utilizes both TOA and MDF methods in conjunction with a lightning waveform recognition algorithm [110]. The sensors are strategically placed around the world but the exact total number of sensors is proprietary information and is unspecified. Each sensor stores a local empirical waveform bank (derived by using a VLF receiver and known lightning location data from NLDN), which catalogs the expected sferic waveform shape, each indexed by distance and ionospheric profile. The most reliable repetitive features (either the rising portion of the ground wave or the zero-crossing of the first or second ionospheric reflection) are used to establish the precise arrival time of the sferic at the receiver. Measured information is sent back to a central processor. All arrival time data are aggregated to make a determination of the event's time and location using an optimization routine that minimizes the root mean squared error from all time and azimuth measurements. The polarity of each stroke is inferred via the cross correlation with the waveform bank. The stroke peak current is deduced from the measured magnetic field, which is first corrected by the source-receiver distance using a propagation model [110]. A lightning event must be simultaneously detected by at least three sensors to be geolocated, though most are detected by more than three. Thunderstorm detection efficiency for the GLD360 is better than 99%, and event timing precision is 1 microsecond RMS. The median location accuracy is 1.5–2.5 km. The present flash detection efficiency is greater than 80% in most areas of the Northern Hemisphere and between 10 and 80% in the Southern Hemisphere, with the lower

efficiencies at latitudes south of 42 S. More detailed information about GLD360 can be found in Said et al. [110, 111].

(13) Earth Networks Total Lightning Network (ENTLN)

The Earth Networks Total Lightning Network (ENTLN) is a unique total lightning detection system specifically targeting the signals emitted from both IC and CG flashes based on over 1700 wideband sensors with frequency reception ranging from 1 Hz to ~12 MHz and now deployed in more than 100 countries worldwide [112]. This system utilizes the TOA technique and extends the frequency range of the sensors into the MF and HF frequency domains, aiming to detect weaker pulses at longer distances than other VLF/LF systems with similar baselines. The sensors record whole waveforms for each flash. The central server employs sophisticated digital signal processing technologies to extract the location, polarity, amplitude, and other stroke parameters from the rich signal measurement. The precise arrival times are calculated by correlating the waveforms from all sensors that detect the strokes of a flash. The type of discharge and polarity are determined by the polarity in the initial half cycle for bipolar pulses and by the waveform in the measured electric field pulse [113]. Strokes (or individual K-change cloud events) are clustered into a flash if they are within 700 ms in time and within 10 km in space of the first detected stroke (or cloud event). The ENTLN processors show a detection efficiency (DE) higher than 99% and 96% for flash and stroke detection, respectively, evaluated using ground truth from natural and rocket-triggered lightning experiments in Florida [114]. More detailed information about the ENTLN can be found in Heckman [115], Liu and Heckman [112], Stock et al. [116], Marchand et al. [117].

(14) Geo-Location and Characterization of Q-burst Transients at ELF Frequencies

At ELF frequencies, the attenuation of the electromagnetic wave propagation in the Earth-ionosphere cavity is sufficiently small (~0.2 dB/Mm) that global resonances are possible, and are now identified as “Schumann resonances”, after their predictor W.O. Schumann [118]. Single lightning flashes of mesoscale extent (>100 km), and often in the form of positive ground flashes, can singlehandedly excite the global Schumann resonance intensities 10–100 times the level of the “background” lightning activity, for periods of one hundred milliseconds or more. Ogawa et al. [119] named these ELF events Q-bursts, because they are relatively Quiet at higher frequencies. These extraordinary flashes can be located globally from a single receiving station equipped with sensors for vertical electric field and horizontal magnetic field.

Theoretical frequency domain representations of the electric E and magnetic H fields throughout a uniform Earth-ionosphere cavity, and produced by a single lightning flash with vertical current moment $I_d S$ (coul-km/sec) are given by Eq. (3)

$$\begin{aligned} E(\omega, \theta) &= \frac{I_d S v(v+1) p_v^0(-\cos \theta)}{4R^2 \epsilon_0 \omega h \sin(\pi v)} \\ H(\omega, \theta) &= \frac{-I_d S p_v^1(-\cos \theta)}{4R h \sin(\pi v)} \end{aligned} \quad (3)$$

where ω is the angular frequency, R is the radius of the Earth, h is the height of the waveguide, ϵ is the permittivity of free space, p is the Legendre function, ν is the complex eigenvalue defining the ionosphere, and θ is the source-receiver angular separation.

So long as the measurements are confined to the lower ELF frequency band from 3 Hz to the waveguide cutoff (1600 Hz at nighttime), only a single TEM waveguide mode is present.

One can eliminate the (unknown) current moment source term IdS by dividing the expression for the E field by the like expression for the H field, to form the wave impedance Z [120], as shown in Eq. (4)

$$Z(\omega, \theta) = E(\omega, \theta)/H(\omega, \theta) = \frac{(\nu + 1) P_{\nu}^0(-\cos \theta)}{R\epsilon\omega P_{\nu}^1(-\cos \theta)} \quad (4)$$

The wave impedance then becomes a meaningful indicator of the source-receiver distance θ , the only other unknown quantity in Eq. (3). Once θ is known, one can recover the current moment IdS from either of Eq. (3). The direction to the source from the receiving station is determined by comparison of two perpendicular calibrated magnetic field antennas, aligned with geographical EW and NS axes. A Poynting vector measurement ($S = E \times H$) can be used to resolve the directional ambiguity along the great circle path inferred from the magnetic direction finding. Given the distance estimate and this great circle bearing, the geographical location of the Q-burst source is uniquely obtained. In this fashion, global lightning maps can be constructed from single station observations [121, 122]. No great locational accuracy can be claimed for this procedure since the relevant EM wavelengths are comparable to the size of the Earth, and the day-night asymmetry of the waveguide (ignored in this application) causes degradation of the linear polarization of the magnetic field that is used for direction finding. Uncertainties in location are of the order of a few hundred km.

The majority of lightning flashes worldwide, and especially the delicate intracloud flashes, do not stand out strongly against the background Schumann resonances, and so cannot be located by the method described above. However, geophysical inversion methods working on the background Schumann resonance spectra recorded at multiple locations [123], [124] can be used to assign an integrated lightning ‘‘activity’’ (in units of $\text{coul}^2 \text{ km}^2/\text{sec}$) for regional ‘‘chimney’’ zones like South America, Africa and the Maritime Continent. This lightning source is expected to have contributions from all lightning flashes, because they all are expected to show some vertical component of charge transfer, given that charge separation in thunderstorms is gravity-driven.

3 Lightning Photography

3.1 Introduction

While detection of lightning events through the propagation of radiated electromagnetic fields is of great value, photographic and video observations also provides us with valuable knowledge about physical lightning processes. In fact, with the advent of modern high-speed video technology, such video studies have become integral to analyzing the structural characteristics and development in time of the lightning process, with thousands of frames per second (*fps*) allowing for the lightning process to be viewed in microseconds. Such observations allow us to clearly view cloud-to-ground lightning events, whether they initiate in the cloud or begin as upward propagating leaders and it is even possible to infer the polarity from such videos. Additionally, when coupled with GPS timestamps, high-speed video studies provide invaluable ground-truth data for comparison with lightning detection and location systems, allowing for detection efficiency and location accuracy to be evaluated.

Using photography to characterize lightning has in fact been attempted since 1926 [125]. Sir Basil Schonland captured images of a lightning leader progression using a two lens streak camera known as a Boys camera (Schonland 1934, [126]). Since then, other studies involving photographing or filming lightning have been conducted involving some initial high-speed technology as well as lower frame rate video recordings [127–130]. Some of the first modern high-speed studies were done by Moreau et al. [131] observing lightning at 200 frames per second. Since then, Ballarotti, Saba and Warner have pioneered high-speed studies of lightning, characterizing both downward and upward lightning flashes, as well as both positive and negative polarities [132–140]. This has led to high-speed studies being conducted around the world [141–145].

3.2 Downward Flashes

Downward flashes are lightning flashes where the leader originates in the cloud and propagates towards the ground. Propagation characteristics are based on the polarity of the flash. Figure 4 shows a frame sequence of a negative downward flash. Negative flashes will appear as branched (or forked) leaders, that continuously branches until one of these branches connects to the ground (Fig. 4a–c). Negative leaders are brighter on the tips than the channel formed during their propagation. The propagation of positive flashes as captured by the cameras will depend on the frame rate used to record. Positive flashes recorded at lower frame rates appear as continuous leaders with no branching; at higher frame rates, repetitive pulses ahead of the leader tip can be seen. Some of these pulses connect and extend the leader propagation towards the ground, and are referred to as recoil leaders. The propagation leader for both positive and negative flashes increases as the leader approaches the ground. From

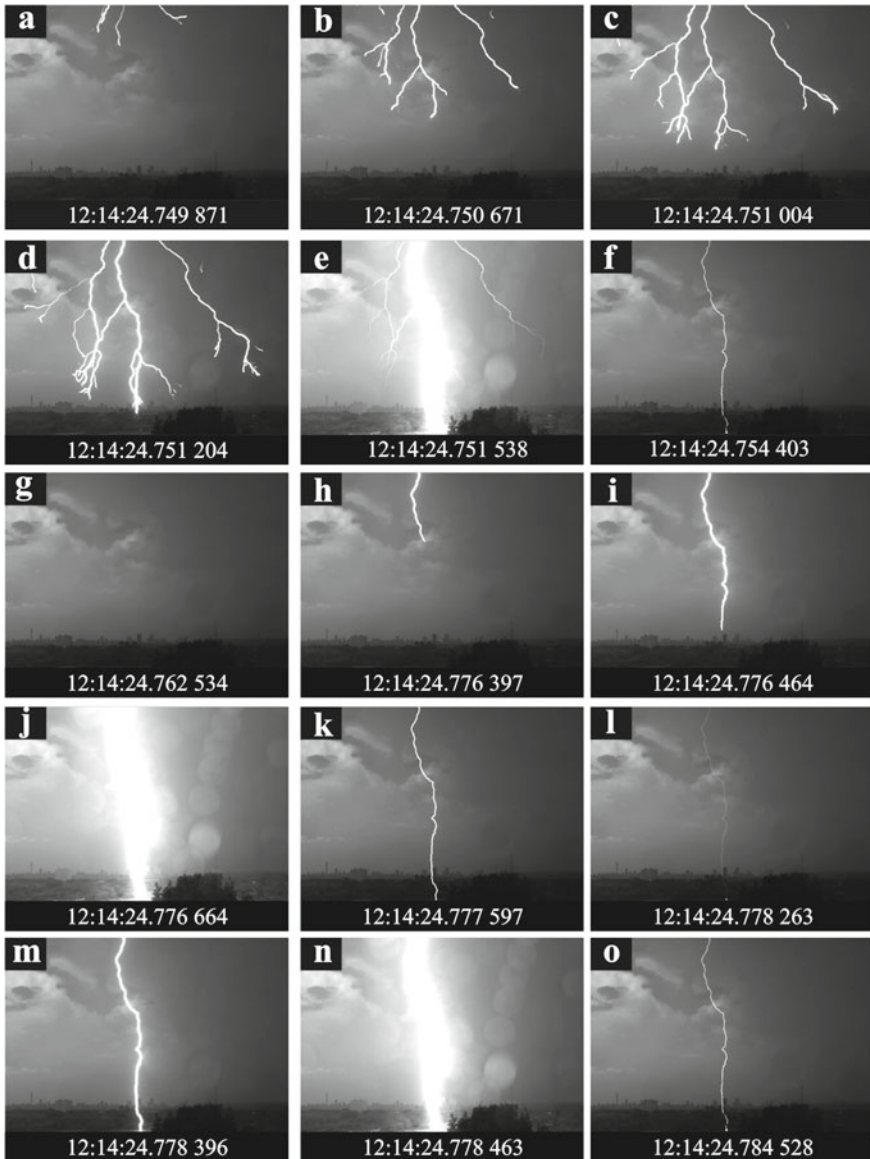


Fig. 4 Photo sequence of a downward flash. Images (a)–(d) show the downward leader approaching the ground; Image (e) shows the return stroke; Image (f) shows the continuing current after the first stroke; Image (g) shows a period of no current prior to the downward leader (h)–(i) that uses the same path to reach the ground and is called the subsequent return stroke (j); Image (k) shows the presence of continuing current in the subsequent return stroke and images (l) and (m) show the current variation and (n) the sudden intense current variation known as the M-component

2D analysis of videos, negative flashes appear to have an average leader speed of $3.30 \times 10^5 \text{ m s}^{-1}$ and positive flashes have an average leader speed of $2.76 \times 10^5 \text{ m s}^{-1}$.

When the leader arrives close to the ground, upward connecting leaders may appear from the potential contact points (Fig. 4d). Only one of these upward connecting leaders will in fact connect and the others will collapse back to ground. These upward connecting leaders are seen to have an average 2D propagation speed from 0.27×10^5 to $2.9 \times 10^5 \text{ m/s}$ before connecting to the downward leader. This connection is known as the return stroke, when thousands of Coulombs are transferred to the ground in a few microseconds. From the camera view, a few very bright frames appear and a fully formed channel is shown in the posterior frames (Fig. 4e and f).

Kitagawa et al. [23], determined that some flashes were able to keep connected to the ground for a longer period than the return stroke. This is seen as a permanence of luminosity in the channel for longer periods and is called continuing current. The continuous luminosity in the photography was correlated with the current through the channel. When there is luminosity, there is charge being transferred between the cloud and the ground. The duration of continuing current can be separated into long (longer than 40 ms), short (between 10 and 40 ms) and very short (between 3 to 10 ms) [23, 60, 146]. The continuing current can be as long as hundreds of milliseconds.

For negative flashes registered in Brazil, 55% of the return strokes were followed by some continuing current [133]. For positive flashes, 97% of the strokes were followed by continuing current (long, short or very short continuing current). To be more specific, 68% of these cases had continuing currents longer than 40 ms [137]. On this continuing current, current pulses may be superimposed and are called M-components (Fig. 4m–o). These superimposed pulses may be detected by lightning location systems.

In addition to the first connection, followed by a continuous current or not, a flash may present a time with no-current followed by a second downward leader using the channel (fully or partially, or even creating a new path) to transfer more charge (called as subsequent return stroke—Fig. 4h–j). Negative flashes commonly have multiple return strokes—on average 3–4 times, and a maximum of 26 subsequent return strokes has been recorded. The majority of positive flashes (84%) only have one and only the return stroke.

The total duration of a flash is considered from the beginning of the first return stroke until the end of the last return stroke (followed by continuous current or not). For negative flashes the median total duration was 163 ms [133]. For positive flashes, the median duration was 125 ms [137]. Negative flashes have longer total duration due to the multiple return strokes, while positive strokes mostly have only one return stroke with long continuous current (Fig. 5).

As the luminosity in the channel is associated with the current flowing between cloud and ground, the luminosity schematics for downward flashes (Fig. 5) represent the different lightning processes and how the channel current varies.

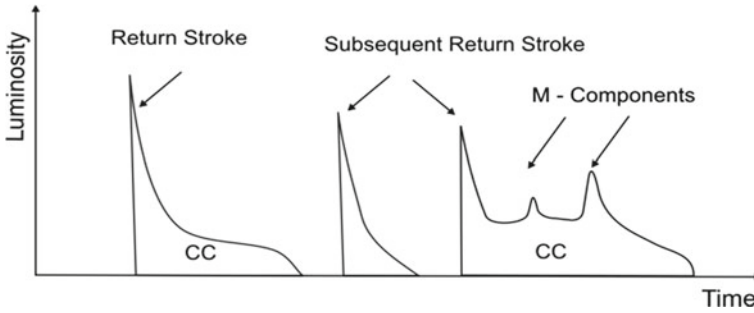


Fig. 5 Luminosity schematics for downward flashes

3.3 Upward Flashes

Upward flashes are flashes that initiate from tall structures and propagate toward the cloud. These flashes may be self-initiated or triggered by nearby lightning activity [145]. The specific component of nearby activities have been determined by recent studies. An intracloud flash, return stroke from a downward flash nearby or a triggering leader over the tower (T-leader) may trigger an upward leader from the tower if it causes enough electric field variation [136, 147]. Figure 6 shows the conditions on the electric field variation to the occurrence of an upward leader from tower tip: self-initiated or triggered by a nearby activity.

When the electric field was reached, an upward leader will initiate from the tower tip towards the cloud base if the electric field variation is enough to pass the critical value of the electric field (E_c). This critical electric field value will be a function of the meteorological conditions (wind, temperature, etc.) and tall structure characteristics (effective height, material, etc.).

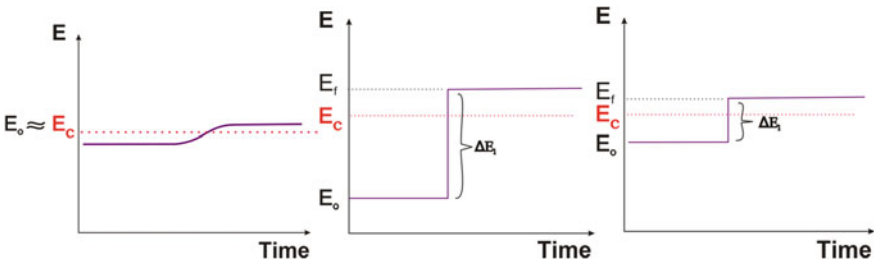


Fig. 6 a *Upward leader self-initiated*: conditions of the initial electric field during thunderstorm are close enough to the electric field critical (E_c) that a slow variation will cause an upward leader from the tall structure. (b1 and b2) *Upward leader triggered by nearby activity*: initial electric field is not enough to cause an upward leader from the tower tip, but due to a fast variation in the electric field nearby (eg. intracloud, return stroke, T-leader) the electric field level surpasses the critical value (E_c). (based on Schumann [136])

For upward flashes, polarities are labelled based on the direction of charge transfer to the ground. Therefore, positive upward flashes will have a negative upward leader propagating towards the cloud base (Fig. 9). Similarly, negative upward flashes will have a positive upward leader propagating toward the cloud base. The propagation leader characteristics will depend on the polarity. Negative upward leaders (Fig. 8) will propagate up with branching as the negative downward flashes do and the positive upward leaders will propagate continuously and may exhibit recoil leaders (repetitive pulses ahead of the leader tip as described in the positive downward flashes leader propagation). These leaders will complete a path, also called a channel (multiple channels in some cases—Fig. 8c), from the tower tip to the cloud, transferring charge. When this process starts with an upward leader and transfers charge between the cloud and the tower, it is called Initial Continuous Current (ICC)—Fig. 8a–k. This process is not fast enough to be detected by most of the lightning detection systems discussed in Sect. 2, although during this transfer some impulsive (ICC Pulses) events may occur and these events can be detected [148]. As shown in the Fig. 8, ICC may have multiple ICC pulses, the first one in Fig. 8 is the sequence (d–f) and the second sequence of ICC pulses (g–i). Even though the connection used different channels, the tower was receiving charge from at least one channel. The duration of the initial continuous current is hundreds of milliseconds and ICC pulses are present in 50% of upward flashes.

Figure 7 shows the luminosity schematic for an upward flash. Sudden events appear brighter in the videos and are more likely to be detected by lightning location network [100]

The majority of the upward flashes consist only of initial continuous current. But when the ICC process finish, a period with no current in the channel can be observed. After a while, a downward leader may use the path to transfer charge. This process is similar to that of subsequent return strokes in the downward flashes (Fig. 8l–o). An upward flash may have multiple return strokes using the same channel of the initial continuous current. Subsequent return strokes are present in 25% of upward flashes [135]. These subsequent return strokes may have M-components (Fig. 8q).

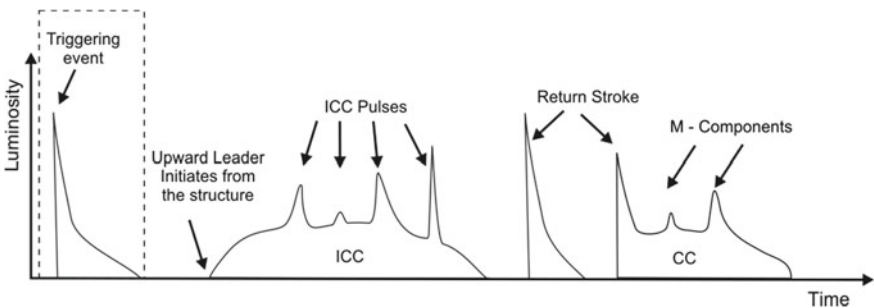


Fig. 7 Luminosity schematics for upward flashes

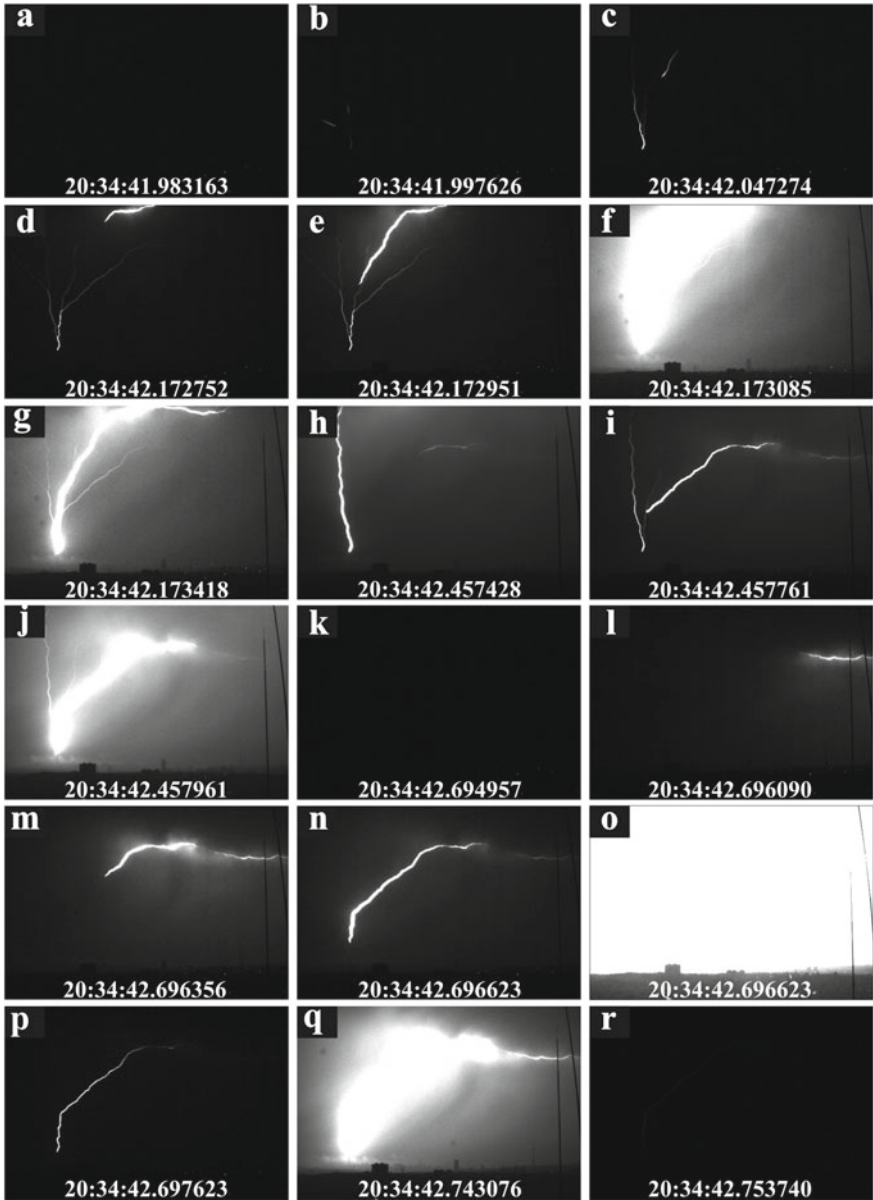


Fig. 8 Photo sequence of a negative upward flash

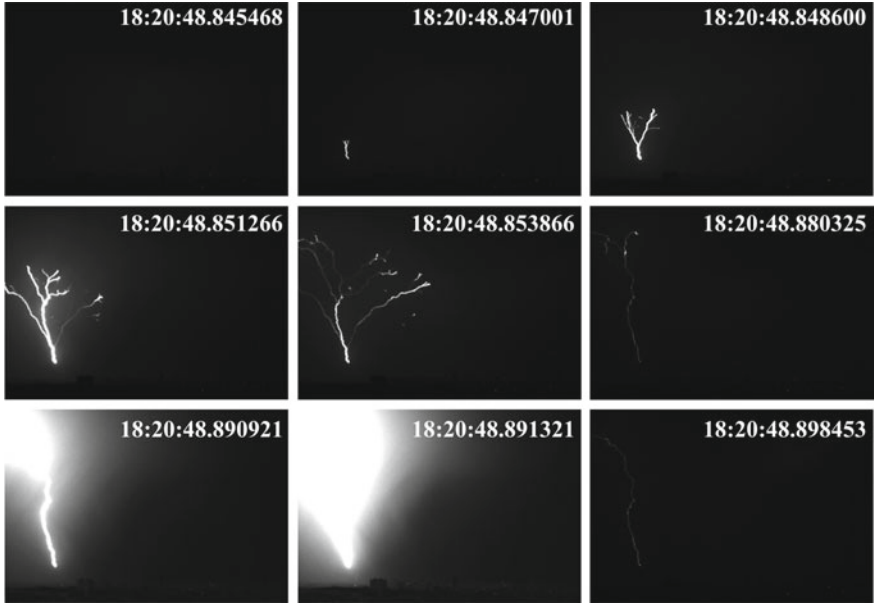


Fig. 9 Negative upward leader

The total average duration of upward flashes is 427 ms (with a maximum of 1143 ms) and is considered from the beginning of the initial continuous current to the end of the continuous current of the last subsequent return stroke [135, 147].

3.4 Comparison with Lightning Detection Networks

As discussed in Sect. 2, the detection of ground lightning flashes through radiated electromagnetic fields relies on multiple sensors detecting the event and then TOA and MDF methods to geolocate the event. As such, it is possible that events may be inaccurately located or not detected at all. Understanding how often this occurs given a detection network is important to understanding the quality of data coming from the network and is referred to as the performance of the network. The performance of a network is usually determined from two parameters: detection efficiency—the number of true lightning events versus the number of detected lightning events and location accuracy—the median error in meters from where true lightning events attached to where the events were reported to have attached.

In order to determine values for such performance criteria, a detection network needs to be compared with ground-truth lightning events. Most notably, rocket-triggered lightning studies in Florida have provided ground-truth cases with a known location to evaluate both detection efficiency and location accuracy [50]. These two

studies showed how the U.S. National Lightning Detection Network improved the flash detection efficiency from 84 to 92% the median location accuracy from 600 to 308 m from 2003 to 2009. Other evaluations have been done with instrumented tall towers—the European Cooperation for Lightning Detection (EUCLID) as regularly evaluated against current measurements made at the Gaisberg tower [74, 149]. High-speed videos with GPS time-stamping provide invaluable ground-truth data for such evaluations as well. Studies in Rapid City, USA by Warner et al. in Brazil by Saba et al., in Austria by Schwartz et al. and by Fensham et al. in South Africa compare lightning detection network reports with high-speed observations of the same lightning events [99, 100, 134, 135, 138, 139, 148, 150].

3.5 Detection Efficiency

A high-speed video study in Johannesburg, South Africa yielded 206 filmed flashes in 24 thunderstorms from February 2017 to February 2018 [100, 147]. This included downward and upward flashes of both polarities. From the high-speed footage, 667 strokes could be seen in the 206 flashes. Each of these flashes was GPS time-stamped meaning the exact timing of every event (stroke, M-component etc.) in each flash is known. The South African Lightning Detection Network (SALDN)—a lightning detection network covering the entirety of South Africa, consisting of 26 Vaisala LS7000 sensors [97]—was then queried for the times of the filmed flashes to correlate the SALDN stroke reports with the ground-truth high-speed video records.

This is shown in Table 1, where can see that 175 of the 206 filmed flashes could time-correlated with SALDN reports (or 457 stroke reports could be time-correlated with the 667 filmed strokes). In other words, the SALDN detected 85% of the filmed flashes and 69% of the filmed strokes. This is to be expected, as a flash only needs

Table 1 Number of SALDN reports correlated with high-speed lightning videos filmed in Johannesburg, South Africa from February 2017 to February 2018 [100, 147]

Lightning events	High speed videos	SALDN detections	Detection efficiency %
Flashes	206	175	85
Strokes	667	457	69
Downward flashes	163	151	93
• Strokes	604	417	69
• M-components	101	12	12
Upward flashes	43	24	56
• Upward leaders	55	0	0
• ICC pulses	387	57	15
• SRSS	63	40	63
• M-components	10	3	30

one stroke to be detected and can be seen in the results presented by Nag et al., where the U.S.NLDN had a flash detection efficiency of 92% but a stroke detection efficiency of 76% compared with rocket-triggered lightning [50]. However, given the detail that can be ascertained about lightning events from high-speed footage, such performance values can be interrogated further. Firstly, the number of downward and upward events can be distinguished—it is often observed that lightning detection networks do not detect upward events as well as downward events due to the slow rise of the initial continuing current. Furthermore, the high-speed video allows us to distinguish M-components from return strokes and subsequent return strokes as well as identify upward leaders and ICC pulses [139, 140, 148].

Table 1 further breaks done the 206 flashes into 163 downward flashes and 43 upward flashes. This distinction already yields interesting results when compared with the SALDN reports with 93 and 56% of the upward flashes being detected. As expected, the detection of upward events is where most of the missed events occurred. The upward events are further described and fractionated as in Fig. 7. Here we once again confirm what was expected, that none of the 55 upward leaders (or initial continuing current) resulted in a detection by the SALDN. However, some of these upward events were detected due to ICC pulses. In other cases, subsequent return strokes occurring after the initial continuing current were detected by the SALDN meaning the upward flash was detected.

Table 2 shows a breakdown of the 43 upward flashes that were filmed. Of these flashes, 16 were followed by subsequent return strokes and 27 were subsequent return strokes (only initial continuing current). 94% of the upward flashes followed by subsequent return strokes were detected whereas only 33% of the upward flashes without subsequent return strokes were detected (due to ICC pulses instead). This confirms the observation that lightning detection networks are able to detect most lightning events, but the slow rise of the initial continuing current leads to non-detected upward flashes.

It is apparent that the detection of subsequent return strokes is key to the ability of a lightning detection network to detect lightning flashes—particularly upward flashes. However, in the case of downward flashes, is it more likely that the first return stroke will be detected than subsequent strokes? And will the multiplicity of a flash mean a higher chance of detection? High-speed video can once again assist in investigating these questions as all first and subsequent return strokes are observable and time-stamped. Figure 10 shows the 163 downward flashes (or 604 strokes) from the study conducted in Johannesburg, South Africa. These are further categorized

Table 2 Upward flash detection efficiency [100, 147]

Lightning event	High speed videos	SALDN detections	Detection efficiency %
Upward flashes	43	24	56
• With SRS	16	15	94
• Without SRS (ICC Only)	27	9	33

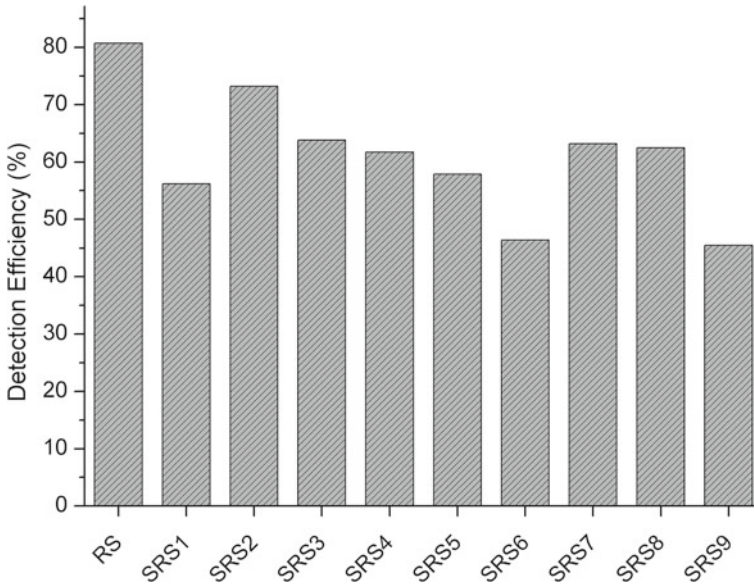


Fig. 10 Detection efficiency of subsequent return strokes. (Adapted from [100])

by subsequent return stroke number—first return stroke (RS), first subsequent return stroke (SRS1), second subsequent return stroke (SRS2) etc. The number of each SRS detected by the SALDN is determined and the stroke detection efficiency is then plotted against the subsequent return stroke order.

It is clear that the first return stroke is detected more often than any of the subsequent return strokes with a detection efficiency of 80%. However, this is not the 93% detection efficiency seen in Table 1 for downward flashes meaning that a number of the downward flash detections are due to subsequent strokes. Interestingly, it appears the first subsequent return stroke (SRS1) is detected less often than the second subsequent return stroke (SRS2).

3.6 Location Accuracy

Ground-truth evidence of lightning attaching to a known location is needed in order to evaluate the location accuracy of a lightning detection network. While high-speed footage of lightning provides excellent ground-truth cases for detection comparisons, it is not always clear where filmed lightning events attached. However, in some cases, particularly events to tall towers, it is clear to see where the lightning channel attached.

The upward lightning flashes filmed in the study by Schumann et al. all initiated from two tall towers in the Johannesburg city center—the Sentech tower and the Hillbrow tower [99, 100, 147]. These are two tall communications towers both

approximately 250 m in height and about 5 km apart. Figure 11 shows a geographical plot of the Johannesburg region. The Sentech and Hillbrow towers are clearly indicated in this figure at 26.1925° South, 28.0068° East and 26.1869° South, 28.0494° East respectively. The location at which the high-speed cameras were placed during the study is also indicated in the plot at 26.1628° South, 27.9598° East, and the field of view is indicated looking South-East through the city with both towers clearly in view.

The figure also shows the reported locations of the SALDN strokes time-correlated with the upward lightning events filmed on the Sentech and Hillbrow towers. As can be seen, a number of reported strokes are clustered around the location of the Sentech tower ($N = 45$) and a number are around the Hillbrow tower ($N = 53$). The cluster around the Sentech tower has a median location error of 75 m with a maximum location error of 1.7 km. Similarly, the cluster around the Hillbrow tower has a median location error of 51 m and a maximum location error of 3.8 km.

In both cases, the maximum error is due to a single stroke outlier, which asks the question—why would one such stroke suddenly be so inaccurately located? We can examine the high-speed footage. Figure 12 shows one frame from the high-speed footage which correlates with the reported time of the stroke reported 1.7 km northwest of the Sentech tower. We can see an intra-cloud (IC) flash as well as an

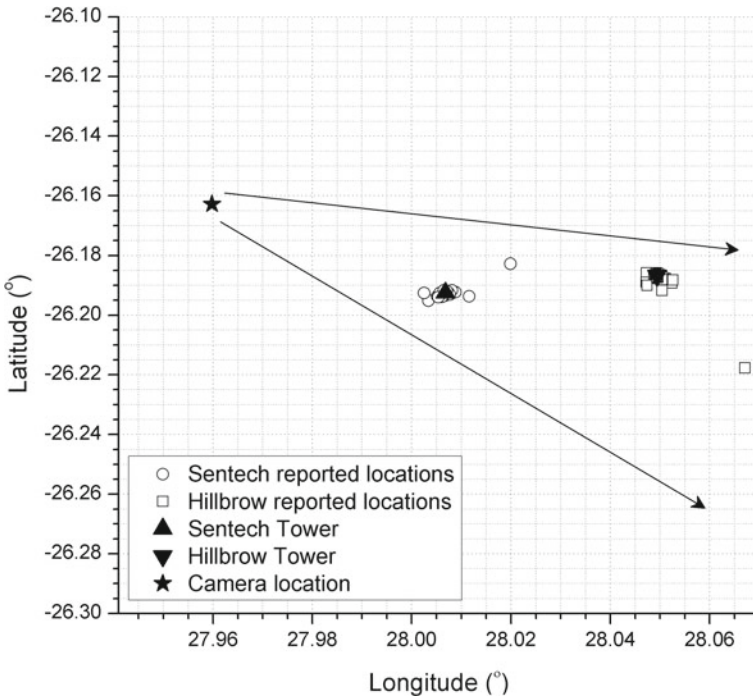


Fig. 11 SALDN reported stroke locations for detections of lightning flashes to the Sentech and Hillbrow towers, Johannesburg, South Africa. (Adapted from [100])

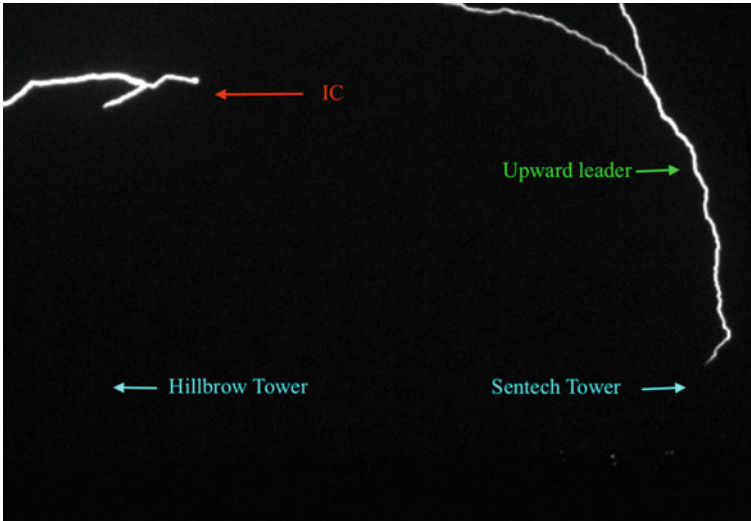


Fig. 12 Image explaining the outlier in the Sentech Tower data [100]

upward leader from the Sentech tower. It appears that this IC flash occurred within the same time that the upward flash was occurring and was therefore classified as part of the upward event. However, from the video footage, it is clear it is a separate flash and appears that the SALDN misclassified an IC event as a CG stroke.

Figure 13 shows a sequence of frames from the video footage time-correlated with the reported time of the SALDN stroke reported 3.8 km South-West of the Hillbrow tower. The upward flash in question was of a negative polarity. In the first image we see an attempted ICC pulse to the Hillbrow Tower. In the second image, a positive subsequent return stroke makes attachment with the attempted ICC pulse in mid-air. The SALDN detected this attachment giving the geographical location of the outlier seen in Fig. 11—to the right of the tower from the perspective of the camera. This agrees with where the attachment took place in the second image in Fig. 13.



Fig. 13 Sequence of images explaining the Hillbrow Tower outlier [100]

4 Thunderstorm Warning by Media and Mobile Apps

4.1 Introduction

Lightning is recognized as one of the most powerful natural hazards. Worldwide, lightning is a more potent killer than any other natural disaster, causing the deaths of at least 6000 people annually, in addition to causing huge damage to livestock and property. In recent years, many laboratory and field experiments have confirmed that a robust relationship exists between lightning flash characteristics and thunderstorm dynamics and other microphysical parameters. Therefore, information on lightning derived from detection networks described in Sect. 2 can be used for meteorological applications such as warning of severe weather and for improving numerical weather prediction. Many agencies have launched many apps aimed at prediction and have successfully provided safety measures to the benefit of society. The main purpose of this section is to decrease deaths and injuries caused by lightning around the world by encouraging gathering and disseminating data to public safety planners, NGOs, policy makers, and others who are in positions to improve safety from lightning for all of their citizens. This section of the chapter will cover methods for reaching the public, particularly the most vulnerable populations, through media and mobile apps.

4.2 Thunderstorm Warning by Media and Mobile Apps

A huge explosion of mobile phone and social media usage has occurred in recent years throughout the developing world. Mobile phones are used for accessing health messages on HIV, child care, and other areas, for information on crops and animal husbandry, for checking market and fuel prices, and for transferring money [151–154]. This mobile phone and social platform may be used effectively for the purpose of thunderstorm warning. The Arab Spring and daily political protests in Venezuela were driven by text messages, Snapchat, and other social media mainly because all other media sources have been shut down [155–157]. In partnership with Airtel, free 3–2–1 service on Human Networks International’s started in Madagascar in 2010 and was generating over 250,000 calls per month by 2015 (HNI.org). These are all examples of person-accessed messages, not broadcast warnings.

4.3 Thunderstorm Warning by Media and Mobile Apps in India

The Indian Institute of Tropical Meteorology (IITM) launched ‘Damini’, a free mobile-based application that can warn people about lightning 30–45 min lead times. Whenever a person is within 20-km radius of a lightning event, the app will send

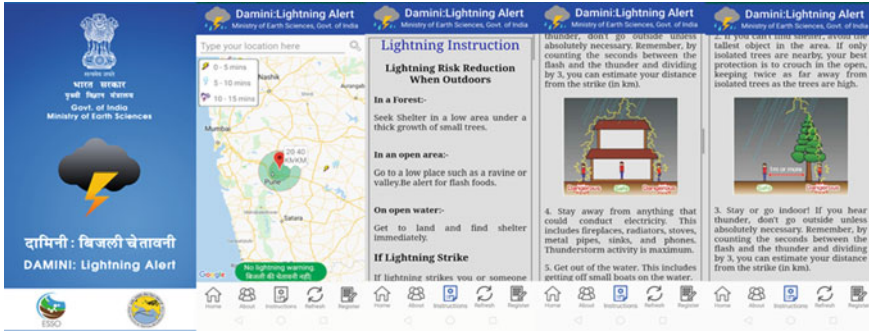


Fig. 14 Sample snapshot from the Damini app showing safety measures to society. With help from this app one may get a warning about lightning hazard within 20 km radius from one’s current location

warnings. The alert can be sent 30 min to 45 min before the event and can help people get to safer locations. The warnings can be given in Hindi and English.

IITM has installed 85-sensor Lightning Location Network over India to investigate the damages caused by lightning over the country. Lightning detection networks use the ‘time of arrival (TOA)’ technique to estimate flash location, as discussed previously in Sect. 2. The network gives some vital information about lightning characteristic such as the location and peak power of lightning. The output from this network is being used to study the relation between different lightning parameters and number of lightning deaths and to generate Lightning alerts which are shared with different authorities dealing with disaster management [158] (Fig. 14).

https://play.google.com/store/apps/details?id=com.lightening.live.damini&hl=en_IN

4.4 Thunderstorm Warning by Other Mobile Apps

In addition to mobile apps developed by Governmental agencies, other commercial and community based warning tools also extend their services to the common people. One such app named ‘WeatherBug’ integrates lightning data from Earth Networks and provides advisories to common people for an impending thunderstorm. The app may be downloaded from the following link.

https://play.google.com/store/apps/details?id=com.aws.android&hl=en_IN

Another community based project www.blitzortung.org serves the same purpose. The mobile app may be downloaded from the link below.

<https://community.windy.com/topic/6605/real-time-lightning-strikes-on-windy-com>

4.5 *Television, Radio, and Print Media*

Television and radio are probably the most effective means of delivering safety messages and other information about lightning and thunderstorms. They require no literacy; the broadcasts are usually free and often in the prevailing language in the area where the safety message is needed. The disadvantage is the frequent unavailability of electricity to power them and the cost of television sets. Radios are much less expensive and more easily battery powered. Everyone recognizes that print media are dying, at least paper versions. Although, the print media may be important for educating people in advance where access to electricity is poor. Effective dissemination is dependent on the popularity of the print venue, literacy, and where the message is located in the publication. If it is buried in the middle of the publication, it is unlikely to be seen.

4.6 *The Challenges*

Trengove and Jandrell [153] posited that the use of mobile phone texting to issue lightning warnings and education would have the following impacts:

1. Reach a large number of people
2. Reach rural people
3. Bridge the digital divide by providing the same service to rich and poor
4. Could use existing mobile telephone infrastructure
5. Could geographically target lightning warning messages.

Some of these hypotheses have been verified, while others are still questionable. Unfortunately, despite decreasing costs in many countries, smartphones remain prohibitively expensive for the poor and rural populations of most countries. Tusshemereirwe and Cooper [159] noted that while 92% of Ugandans surveyed had mobile phones, only 4% had smartphones. Floods, drought, and severe storms tend to disproportionately affect women since they are more commonly responsible for farm labor, food security, and household management in developing countries. The majority of farmers in Uganda are women, yet gender disparities limit their access to information on which to base decisions and adjust to climate shocks [160]. This circumstance is caused by women's restricted access to technology and communication channels, by lower education levels, and by culturally defined roles in household chores such as raising children and cooking. In Africa, women are 23% less likely to own a mobile phone than are men [161]. Financial barriers such as the inability to pay fees or even to own a mobile phone or radio can leave them uninformed of weather-related impacts. Airtime can be expensive and unreliable. Electricity may be available only erratically, leading to mismatches between a person or home's allotted electricity window and the internet provider's window. As in most countries, there are multiple airtime providers so that not all of the population would likely be covered, and it would require funding by each company. For the HNI-Airtel partnership mentioned earlier, HNI, through private funding, provides the translated messages and Airtel

provides a monthly allowance of free calls to promote customer loyalty. Not all telephone services are this benevolent [162].

Of course, targeted warnings in either of these settings would depend on GPS coordinates, reliable and consistent internet or cell phone availability, how long thunderstorms last in this region, and the speed of movement of a thunderstorm. Additional factors include the quality and timeliness of the forecast and the willingness and funding of the meteorological service to implement such a system.

References

1. Chalmers JA (1967) Atmospheric electricity, 2nd Edition, Elsevier
2. Kelvin L (1884) Reprints on papers in electrostatics and magnetism. MacMillan and Company
3. Rust WD, MacGorman DR (1987) Techniques for measuring electrical parameters of thunderstorms, Chapter 8. In: Kessler E (Editor) Instruments and techniques for thunderstorm observation and analysis, vol 3, University of Oklahoma Press
4. Mazur V (2016) Principles of lightning physics. IOP Publishing
5. Uman MA (2001) The lightning discharge. Courier Corporation
6. Berger K (1967) Novel observations on lightning discharges: Results of research on Mount San Salvatore. *J Franklin Inst* 283(6):478–525
7. Cooray GV (2009) Lightning protection. *Inst Eng Technol*
8. Uman MA, Krider EP (1989) Natural and artificially initiated lightning. *Science* 246:457–464
9. Williams E (2020) Lightning and climate change, Chapter 1 of lightning interaction with power systems. In: Piantini A (ed) Fundamentals and modelling, vol 1
10. Uman MA (2012) Lightning. Courier Corporation
11. Cummins KL, Murphy MJ, Bardo EA, Hiscox WL, Pyle RB, Pifer AE (1998) A combined TOA/MDF technology upgrade of the US National Lightning Detection Network. *J Geophys Res Atmos* 103(D8):9035–9044
12. Dwyer JR, Rassoul HK, Al-Dayeh M, Caraway L, Chrest A, Wright B, Kozak E, Jerauld J, Uman MA, Rakov VA, Jordan DM, Rambo KJ (2005) X-ray bursts associated with leader steps in cloud-to-ground lightning. *Geophys Res Lett* 32(1):1–4
13. Rakov VA, Uman MA (2003) Lightning: physics and effects. Cambridge University Press
14. Clarence ND, Malan DJ (1957) Preliminary discharge processes in lightning flashes to ground. *Q J R Meteorol Soc* 83(356):161–172
15. Campos LZ, Saba MM, Warner TA, Pinto O Jr, Krider EP, Orville RE (2014) High-speed video observations of natural cloud-to-ground lightning leaders-A statistical analysis. *Atmos Res* 135:285–305
16. Krider EP, Weidman CD, Noggle RC (1977) The electric fields produced by lightning stepped leaders. *J Geophys Res* 82(6):951–960
17. Warner TA (2012) Observations of simultaneous upward lightning leaders from multiple tall structures. *Atmos Res* 117:45–54
18. Idone VP, Orville RE (1982) Lightning return stroke velocities in the thunderstorm research international program (TRIP). *J Geophys Res Oceans* 87(C7):4903–4916
19. Cooray GV (2013) The lightning flash (No. 34). IET Digital Libr
20. Krider EP, Noggle RC, Pifer AE, Vance DL (1980) Lightning direction-finding systems for forest fire detection. *Bull Am Meteor Soc* 61(9):980–986
21. Kitagawa N (1957) On the mechanism of cloud flash and junction or final process in flash to ground. *Pap Meteorol Geophys* 7(4):415–424
22. Jordan DM, Idone VP, Rakov VA, Uman MA, Beasley WH, Jurenka H (1992) Observed dart leader speed in natural and triggered lightning. *J Geophys Res Atmos* 97(D9):9951–9957

23. Kitagawa N, Brook M, Workman EJ (1962) Continuing currents in cloud-to-ground lightning discharges. *J Geophys Res* 67(2):637–647
24. Malan DJ, Schonland BFF (1947) Progressive lightning. VII Directly-correlated photographic and electrical studies of lightning from near thunderstorms. *Proc R Soc London. Ser Math Phys Sci* 191(1027):485–503
25. Thottappillil R, Rakov VA, Uman MA (1990) K and M changes in close lightning ground flashes in Florida. *J Geophys Res Atmos* 95(D11):18631–18640
26. Goodman SJ, Blakeslee RJ, Koshak WJ, Mach D, Bailey J, Buechler D, Carey L, Schultz C, Bateman M, McCaul E Jr, Stano G (2013) The GOES-R geostationary lightning mapper (GLM). *Atmos Res* 125:34–49
27. Jacobson AR, Shao XM, Holzworth RH (2011) Satellite triangulation of thunderstorms, from fading radio fields synchronously recorded on two orthogonal antennas. *Radio Sci* 46(06):1–17
28. Kotaki M, Katoh C (1983) Global distribution of atmospheric radio noise derived from distribution of lightning activity. *Radio Res Lab J* 30:35–57
29. Morimoto T, Kikuchi H, Sato M, Suzuki M, Yamazaki A, Ushio T (2011) VHF lightning observations on JEM-GLIMS mission. *IEEJ Trans Fundam Mater* 131(12):977–982
30. Boeck WL, Suszcynsky DM, Light TE, Jacobson AR, Christian HJ, Goodman SJ, Buechler DE, Guillen JLL (2004) A demonstration of the capabilities of multisatellite observations of oceanic lightning. *J Geophys Res Atmos* 109(D17):1–8
31. Jacobson AR, Knox SO, Franz R, Enemark DC (1999) FORTE observations of lightning radio-frequency signatures: Capabilities and basic results. *Radio Sci* 34:337–354
32. Jernegan MW (1928) Benjamin Franklin’s “electrical kite” and lightning rod. *N Engl Q* 1(2):180–196
33. Norinder H (1953) Long distance location of thunderstorms. *Thunderstorm Electricity*, 276–327
34. Blois De (1914) *Amer InstElec Eng* 33:563–579
35. Watt RW, Appleton EV (1923) On the nature of atmospherics. I. *Proc R Soc London. Ser Containing Pap Math Phys Charact* 84–102
36. Cummins KL, Murphy MJ (2009) An overview of lightning locating systems: History, techniques, and data uses, with an in-depth look at the US NLDN. *IEEE Trans Electromagn Compat* 51(3):499–518
37. Cianos N, Oetzel GN, Pierce ET (1972) A technique for accurately locating lightning at close ranges. *J Appl Meteorol* 11(7):1120–1127
38. Maier L, Lennon C, Britt T, Schaefer S (1995) LDAR system performance and analysis. In: *Proceedings of the international conference on cloud physics*. Am Meteorol Soc, Dallas, Tex
39. Rhodes CT, Shao X-M, Krehbiel PR, Thomas RJ, Hayenga CO (1994) Observations of lightning phenomena using radio interferometry. *J Geophys Res* 99:13059–13082
40. Shao XM, Krehbiel PR, Thomas RJ, Rison W (1995) Radio interferometric observations of cloud-to-ground lightning phenomena in Florida. *J Geophys Res* 100:2749–2783.
41. Rison W, Thomas RJ, Krehbiel PR, Hamlin T, Harlin J (1999) A GPS-based three-dimensional lightning mapping system: initial observations in central New Mexico. *Geophys Res Lett* 26(23):3573–3576
42. Krehbiel PR, Thomas R, Rison W, Hamlin T, Harlin J, Davis M (1998) Lightning mapping observations during MEaPRS in central Oklahoma. *EOS Trans AGU* 79:F127
43. Thomas RJ, Krehbiel PR, Rison W, Hamlin T, Boccippio DJ, Goodman SJ, Christian HJ (2000) Comparison of ground-based 3-dimensional lightning mapping observations with satellite-based LIS observations in Oklahoma. *Geophys Res Lett* 27(12):1703–1706
44. Thomas RJ, Krehbiel PR, Rison W, Hunyady SJ, Winn WP, Hamlin T, Harlin J (2004) Accuracy of the lightning mapping array. *J Geophys Res Atmos* 109(D14)
45. Orville RE (1994) Cloud-to-ground lightning flash characteristics in the contiguous United States: 1989–1991. *J Geophys Res Atmos* 99(D5):10833–10841
46. Orville RE, Huffines GR (2001) Cloud-to-ground lightning in the United States: NLDN results in the first decade, 1989–98. *Mon Weather Rev* 129(5):1179–1193

47. Biagi CJ, Cummins KL, Kehoe KE, Krider EP (2007) NLDN performance in Southern Arizona, Texas and Oklahoma in 2003–2004. *J Geophys Res* 112:D05208
48. Fleenor SA, Biagi CJ, Cummins KL, Krider EP, Shao XM (2009) Characteristics of cloud-to-ground lightning in warm-season thunderstorms in the Central Great Plains. *Atmos Res* 91:333–352
49. Jerauld J, Rakov VA, Uman MA, Rambo KJ, Jordan DM, Cummins KL, Cramer JA (2005) An evaluation of the performance characteristics of the U.S. National Lightning Detection Network in Florida using rocket-triggered lightning. *J Geophys Res Atmos* 110(D19)
50. Nag A, Mallick S, Rakov VA, Howard JS, Biagi CJ, Hill JD, Uman MA, Jordan DM, Rambo K, Jerauld JJE, Decarlo BA, Cummins KL, Cramer JA (2014) Evaluation of U.S. national lightning detection network performance characteristics using rocket-triggered lightning data acquired in 2004–2009. *J Geophys Res Atmos* 116(D2)
51. Orville RE, Huffines GR, Burrows WR, Holle RL, Cummins KL (2002) The North American lightning detection network (NALDN)—First results: 1998–2000. *Mon Weather Rev* 130(8):2098–2109
52. Orville RE, Huffines GR, Burrows WR, Cummins KL (2011) The North American lightning detection network (NALDN)—Analysis of flash data: 2001–09. *Mon Weather Rev* 139(5):1305–1322
53. Holle RL (2014) Diurnal variations of NLDN-reported cloud-to-ground lightning in the United States. *Mon Weather Rev* 142(3):1037–1052
54. Abreu D, Chandan D, Holzworth RH, Strong K (2010) A performance assessment of the World Wide Lightning Location Network (WWLLN) via comparison with the Canadian Lightning Detection Network (CLDN). *Atmos Meas Tech* 3(4):1143–1153
55. Burrows WR, King P, Lewis PJ, Kochtubajda B, Snyder B, Turcotte V (2002) Lightning occurrence patterns over Canada and adjacent United States from lightning detection network observations. *Atmos Ocean* 40(1):59–80
56. Dockendorff D, Spring K (2005) The Canadian lightning detection network—novel approaches for performance measurement and network management. In: *Proceedings, WMO technical conference on instruments and methods of observation (TECO)*. Bucharest, Romania
57. Shostak V, Bormotov O, Pavanello D, Janischewskyj W, Rachidi F (2012) Analysis of lightning detection network data for selected areas in Canada. In: *2012 international conference on lightning protection (ICLP)*. IEEE, pp 1–12
58. Kazazi S, Hussein AM, Liatos P (2015) Evaluation of the performance characteristics of the North American Lightning Detection Network based on recent CN Tower lightning data. In: *2015 international symposium on lightning protection (XIII SIPDA)*. IEEE, pp 327–333
59. Ballarotti MG, Saba MMF, Pinto Jr O (2006) A new performance evaluation of the Brazilian Lightning Location System (RINDAT) based on high-speed camera observations of natural negative ground flashes. In: *19th international lightning detection conference*, Vaisala, Tucson, Arizona
60. Ballarotti MG, Saba MMF, Pinto Jr O (2005) High-speed camera observations of negative ground flashes on a millisecond-scale. *Geophys Res Lett* 32(23)
61. Pinto Jr O (2005) *The art of war against lightning* (in Portuguese), Oficina de Texto Press
62. Solorzano NN (2003) *Triggered lightning study in Brazil*. Ph.D. Thesis, INPE, 178 p (in Portuguese)
63. Pinto Jr O (2003) *The Brazilian lightning detection network: a historical background and future perspectives*, paper presented at VII International Symposium on Lightning Protection (SIPDA), Inst.de Eletr. e Energ., Curitiba, Brazil
64. Pinto Jr O, Pinto IRCA, Gomes MASS, Vitorello I, Padilha AL, Diniz JH, Carvalho AM, Filho AC (1999) Cloud-to-ground lightning in southeastern Brazil in 1993: 1. Geographical distribution. *J Geophys Res Atmos* 104 (D24):31369–31379
65. Pinto O Jr, Naccarato KP, Pinto IRCA, Fernandes WA, Neto OP (2006a) Monthly distribution of cloud-to ground lightning flashes as observed by lightning location systems. *Geophys Res Lett* 33(9):1–4

66. Pinto Jr O, Naccarato KP, Saba MMF, Pinto IRCA, Abdo RF, Garcia SDM, Cazetta Filho A (2006b) Recent upgrade to the Brazilian integrated lightning detection network. In: Proceedings of the 19th international lightning detection conference (ILDC). Tucson, AZ
67. Betz HD, Schmidt K, Oettinger WP (2009a) LINET-An international VLF/LF lightning detection network in Europe. In: *Lightning: principles, instruments and applications*. Springer, Dordrecht, pp 115–140
68. Betz HD, Schmidt K, Laroche P, Blanchet P, Oettinger WP, Defer E, Dziewit Z, Konarski J (2009b) LINET-An international lightning detection network in Europe. *Atmos Res* 91(2–4):564–573
69. Betz HD, Meneux B (2014) LINET systems-10 years experience. In: 2014 international conference on lightning protection (ICLP), pp 1553–1557
70. Betz HD, Schumann U, Laroche P (eds) (2008) *Lightning: principles, instruments and applications: Review of modern lightning research*. Springer Science & Business Media, Berlin
71. Azadifar M, Rachidi F, Rubinstein M, Paolone M, Diendorfer G, Pichler H, Schulz W, Pavanello D, Romero C (2016) Evaluation of the performance characteristics of the European Lightning Detection Network EUCLID in the Alps region for upward negative flashes using direct measurements at the instrumented Säntis Tower. *J Geophys Res Atmos* 121(2):595–606
72. Schulz W, Cummins K, Diendorfer G, Dorninger M (2005) Cloud-to-ground lightning in Austria: A 10-year study using data from a lightning location system. *J Geophys Res Atmos* 110(D9)
73. Romero C, Paolone M, Rachidi F, Rubinstein M, Rubinstein A, Diendorfer G, Schulz W, Bernardi M, Nucci CA (2011) Preliminary comparison of data from the säntis tower and the EUCLID lightning location system. In: 2011 international symposium on lightning protection. IEEE, pp 140–145
74. Schulz W, Diendorfer G, Pedebay S, Poelman DR (2016) The European lightning location system EUCLID part 1: Performance analysis and validation. *Nat Hazard* 16(2):595–605
75. Pohjola H, Mäkelä A (2013) The comparison of GLD360 and EUCLID lightning location systems in Europe. *Atmos Res* 123:117–128
76. Poelman DR, Schulz W, Kaltenboeck R, Delobbe L (2017) Analysis of lightning outliers in the EUCLID network. *Atmos Meas Tech* 10(11)
77. Biron D (2009) LAMPINET-lightning detection in Italy. In: *Lightning: principles, instruments and applications*, Springer, Dordrecht, pp 141–159
78. Biron D, De Leonibus L, Betz HD (2007) Campaign, with locations produced by two different detection network in Central Europe: LAMPINET and LINET. European Geosciences Union, 2007. In: *Geophysical research abstracts*, 9, 02500
79. Biron CD, De Leonibus LCL, Zauli LCF (2006) The lightning network LAMPINET of the Italian Air Force Meteorological Service. In: *Proceeding of 19th international lightning detection conference*. Tucson, USA
80. García Mollá PJ (1910) *La section électrique, Mèmoires de l'Observatoire de l'Èbre*, Ed. Gustavo Gili, Barcelona
81. Pineda N, Montanyà J (2009) Lightning detection in Spain: the particular case of Catalonia. In: *Lightning: principles, instruments and applications*. Springer, Dordrecht, pp 161–185
82. Pérez PF, Rodríguez CZ (AEMET) (2008) La frecuencia de las tormentas eléctricas en España. *Bol de la quinta etapa de la Asoc Meteorológica Esp* 21:37–44
83. Montanyà J, Pineda N, March V, Illa A, Romero D, Solà G (2006) Experimental evaluation of the Catalan lightning detection network. In: 19th international lightning detection conference, Tucson, Apr 2006
84. Pineda N, Rigo T, Bech J, Soler X (2007) Lightning and precipitation relationship in summer thunderstorms: case studies in the North Western Mediterranean region. *Atmos Res* 85(2):159–170
85. Li YJ, Zhang GS, Wang YH, Wu B, Li J (2017) Observation and analysis of electrical structure change and diversity in thunderstorms on the Qinghai-Tibet Plateau. *Atmos Res* 194:130–141

86. Zhang GS, Wang YH, Qie XS, Zhang T, Zhao YX, Li YJ, Cao DJ (2010) Using lightning locating system based on time-of-arrival technique to study three-dimensional lightning discharge processes. *Sci China Earth Sci* 53(4):591–602
87. Li YJ, Zhang GS, Wen J, Wang DH, Wang YH, Zhang T, Fan XP, Wu B (2013) Electrical structure of a Qinghai-Tibet Plateau thunderstorm based on three-dimensional lightning mapping. *Atmos Res* 134:137–149
88. Wang Y, Qie X, Wang D, Liu M, Su D, Wang Z, Liu D, Wu Z, Sun Z, Tian Y (2015) Beijing Lightning NETwork (BLNET): Configuration and preliminary results of lightning location. *Chin J Atmos Sci* 39(3):571–582
89. Srivastava A, Tian Y, Qie X, Wang D, Sun Z, Yuan S, Wang Y, Chen Z, Xu W, Zhang H, Jiang R (2017) Performance assessment of Beijing Lightning Network (BLNET) and comparison with other lightning location networks across Beijing. *Atmos Res* 197:76–83
90. Liu H, Qiu S, Dong W (2018) The three-dimensional locating of VHF broadband lightning interferometers. *Atmosphere* 9(8):317–331
91. Chen LW, Zhang YJ, Lu WT, Zheng D, Zhang Y, Chen SD, Huang ZH (2012) Performance evaluation for a lightning location system based on observations of artificially triggered lightning and natural lightning flashes. *J Atmos Oceanic Tech* 29:1835–1844
92. Zhang H, Lu G, Qie X, Jiang R, Fan Y, Tian Y, Sun Z, Liu M, Wang Z, Liu D, Feng G (2016) Locating narrow bipolar events with single-station measurement of low-frequency magnetic fields. *J Atmos Solar Terr Phys* 143:88–101
93. Lyu W, Ma Y, Qi Q, Chen L, Wu B, Su Z, Wu S (2018) Lightning optical observation at TOLOG. In: 34th international conference on lightning protection (ICLP). IEEE, pp 1–4
94. Wu B, Lyu W, Qi Q, Ma Y, Chen L, Zhang Y, Zhu Y, Rakov VA (2019) Synchronized two-station optical and electric field observations of multiple upward lightning flashes triggered by a 310-kA+ CG flash. *J Geophys Res Atmos* 124(2):1050–1063
95. Qie X, Zhang Y, Yuan T, Zhang Q, Zhang T, Zhu B, Lu W, Ma M, Yang J, Zhou Y, Feng G (2015) A review of atmospheric electricity research in China. *Adv Atmos Sci* 32(2):169–191
96. Shi D, Zheng D, Zhang Y, Zhang Y, Huang Z, Lu W, Chen S, Yan X (2017) Low-frequency E-field detection array (LFEDA)-construction and preliminary results. *Sci China Earth Sci* 60(10):1896–1908
97. Gijben M (2012) The lightning climatology of South Africa. *S Afr J Sci* 108(3–4):44–53
98. Gill T (2008) A lightning climatology of South Africa for the first two years of operation of the South African Weather Service Lightning Detection Network: 2006–2007. In: 20th international lightning detection conference, pp 1–12
99. Fensham HG, Schumann C, Hunt HGP, Nixon KJ, Warner TA, Gijben M (2018) Performance evaluation of the SALDN using high-speed camera footage of ground truth lightning events over Johannesburg, South Africa. In: 34th international conference on lightning protection (ICLP). Rzeszow, Poland
100. Fensham HG (2019) Performance evaluation of the SALDN using high-speed camera footage. Master Dissertation, University of the Witwatersrand
101. Hunt H, Liu YC, Nixon K (2014) Evaluation of the South African Lightning Detection Network using photographed tall tower lightning events from 2009–2013. In: 32nd international conference on lightning protection (ICLP). Shanghai, China
102. Dowden RL, Brundell JB, Rodger CJ (2002) VLF lightning location by time of group arrival (TOGA) at multiple sites. *J Atmos Solar Terr Phys* 64(7):817–830
103. Abarca SF, Corbosiero KL, Galarneau Jr TJ (2010) An evaluation of the worldwide lightning location network (WWLLN) using the national lightning detection network (NLDN) as ground truth. *J Geophys Res Atmos* 115(D18):2010
104. Hutchins ML, Holzworth RH, Brundell JB, Rodger CJ (2012) Relative detection efficiency of the World Wide Lightning Location Network. *Radio Sci* 47(6):1–9
105. Jacobson AR, Holzworth R, Harlin J, Dowden R, Lay E (2006) Performance assessment of the world wide lightning location network (WWLLN), using the Los Alamos spheric array (LASA) as ground truth. *J Atmos Oceanic Tech* 23(8):1082–1092

106. Rodger CJ, Werner S, Brundell JB, Lay EH, Thomson NR, Holzworth RH, Dowden RL (2006) Detection efficiency of the VLF World-Wide Lightning Location Network (WWLLN): initial case study. *Ann Geophys* 24(12):3197–3214
107. Mezuman K, Price C, Galanti E (2014) On the spatial and temporal distribution of global thunderstorm cells. *Environ Res Lett* 9(12):124023
108. Virts KS, Wallace JM, Hutchins ML, Holzworth RH (2013) Highlights of a new ground-based, hourly global lightning climatology. *Bull Am Meteor Soc* 94(9):1381–1391
109. Lay EH, Holzworth RH, Rodger CJ, Thomas JN, Pinto O Jr, Dowden RL (2004) WWLLN global lightning detection system: regional validation study in Brazil. *Geophys Res Lett* 31(3):1–5
110. Said RK, Inan US, Cummins KL (2010) Long-range lightning geolocation using a VLF radio atmospheric waveform bank. *J Geophys Res Atmos* 115(D23)
111. Said RK, Cohen MB, Inan US (2013) Highly intense lightning over the oceans: Estimated peak currents from global GLD360 observations. *J Geophys Res Atmos* 118(13):6905–6915
112. Liu CL, Heckman S (2011) The application of total lightning detection and cell tracking for severe weather prediction. In: 91st annual meeting of the American meteorological society. pp 1–10
113. Mallick S, Rakov VA, Hill JD, Ngien T, Gamerota WR, Pilkey JT, Jordan DM, Uman MA, Heckman S, Liu C (2015) Performance characteristics of the ENTLN evaluated using rocket-triggered lightning data. *Electr Power Syst Res* 118:15–28
114. Zhu Y, Rakov VA, Tran MD, Stock MG, Heckman S, Liu C, Sloop CD, Jordan DM, Uman MA, Caicedo JA, Kotovsky DA (2017) Evaluation of ENTLN performance characteristics based on the ground truth natural and rocket-triggered lightning data acquired in Florida. *J Geophys Res Atmos* 122(18):9858–9866
115. Heckman S (2014) ENTLN status update. In: XV international conference on atmospheric electricity, 15–20 June 2014
116. Stock M, Lapierre J, Heckman S, Borges M, Anderson J (2017) Estimating detection efficiency in the absence of satellites: ENTLN detection efficiency in 2015 and 2016. In: IEEE international symposium on lightning protection (XIV SIPDA), pp 333–335
117. Marchand M, Hilburn K, Miller SD (2019) Geostationary lightning mapper and earth networks lightning detection over the contiguous United States and dependence on flash characteristics. *J Geophys Res Atmos* 124(11):552–567
118. Schumann WO (1952) Über die strahlungslosen Eigenschwingungen einer leitenden Kugel, die von einer Luftschicht und einer Ionosphärenhülle umgeben ist. *Z. Naturforsch.*, 7a, 149
119. Ogawa T, Tanaka Y, Miura T, Yasuhara M (1966) Observations of natural ELF and VLF electromagnetic noises by using ball antennas. *J Geomagn Geoelectr* 18(4):443–454
120. Kemp DT, Jones DL (1971) A new technique for the analysis of transient ELF electromagnetic disturbances within the Earth-ionosphere cavity. *J Atmos Terr Phys* 33(4):567–572
121. Hobara Y, Hayakawa M, Williams E, Boldi R, Downes E (2006) Location and electrical properties of sprite-producing lightning from a single ELF site. In: Sprites, elves and intense lightning discharges. Springer, Dordrecht, pp 211–235
122. Huang E, Williams E, Boldi R, Heckman S, Lyons W, Taylor M, Nelson T, Wong C (1999) Criteria for sprites and elves based on Schumann resonance observations. *J Geophys Res Atmos* 104(D14):16943–16964
123. Williams E, Mareev E (2014) Recent progress on the global electrical circuit. *Atmos Res* 135:208–227
124. Prácsér E, Bozóki T, Sători G, Williams E, Guha A, Yu H (2019) Reconstruction of global lightning activity based on Schumann Resonance measurements: Model description and synthetic tests. *Radio Sci* 54(3):254–267
125. Boys CV (1926) Progressive lightning. *Nature* 118:749–750
126. Schonland BFJ (1956) The lightning discharge. *Hand Phys* 22:576–628
127. Brantley RD, Tiller JA, Uman MA (1975) Lightning properties in Florida thunderstorms from video tape records. *J Geophys Res* 80(24):3402–3406

128. Jordan DM, Rakov VA, Beasley WH, Uman MA (1997) Luminosity characteristics of dart leaders and return strokes in natural lightning. *J Geophys Res Atmos* 102(D18):22025–22032
129. Waldeuff P, Metzger P, Boulay JL, Laroche P, Hubert P (1980) Triggered lightning strokes originating in clear air. *Journal of Geophysical Research: Oceans* 85(C5):2861–2868
130. Winn WP, Aldridge TV, Moore CB (1973) Video tape recordings of lightning flashes. *J Geophys Res* 78:4515–4519
131. Moreau JP, Alliot JC, Mazur V (1992) Aircraft lightning initiation and interception from in situ electric measurements and fast video observations. *J Geophys Res Atmos* 97(D14):15903–15912
132. Ballarotti MG, Medeiros C, Saba MM, Schulz W, Pinto O Jr (2012) Frequency distributions of some parameters of negative downward lightning flashes based on accurate-stroke-count studies. *J Geophys Res Atmos* 117(D6):1–8
133. Saba MMF, Ballarotti MG, Pinto Jr O (2006) Negative cloud-to-ground lightning properties from high-speed video observations. *J Geophys Res Atmos* 111(D3)
134. Saba MM, Schulz W, Warner TA, Campos LZ, Schumann C, Krider EP, Cummins KL, Orville RE (2010) High-speed video observations of positive lightning flashes to ground. *J Geophys Res Atmos* 115(D24)
135. Saba MM, Schumann C, Warner TA, Ferro MAS, de Paiva AR, Helsdon J Jr, Orville RE (2016) Upward lightning flashes characteristics from high-speed videos. *J Geophys Res Atmos* 121(14):8493–8505
136. Schumann C (2016) Estudo dos raios ascendentes a partir de observações de câmeras de alta resolução temporal e de medidas de campo elétrico—Ph.D. thesis 2016
137. Schumann C (2012) Caracterização dos raios positivos através de câmeras de alta velocidade e sensores de campo elétrico, Master's dissertation, Department of Space Geophysic, Atmospheric Electricity Group, National Institute for Space Research, São José dos Campos, Brazil
138. Warner TA, Saba MMF, Rudge S, Bunkers M, Lyons WA, Orville RE (2012a) Lightning-triggered upward lightning from towers in Rapid City, South Dakota. In: 2012 International lightning detection conference. Boulder, Colorado
139. Warner TA, Cummins KL, Orville RE (2012b) Upward lightning observations from towers in Rapid City, South Dakota and comparison with National Lightning Detection Network data, 2004–2010. *J Geophys Res Atmos* 117(D19)
140. Warner TA, Saba MM, Schumann C, Helsdon JH Jr, Orville RE (2016) Observations of bidirectional lightning leader initiation and development near positive leader channels. *J Geophys Res Atmos* 121(15):9251–9260
141. Flache D, Rakov VA, Heidler F, Zischank W, Thottappillil R (2008) Initial-stage pulses in upward lightning: leader/return stroke versus M-component mode of charge transfer to ground. *Geophys Res Lett* 35(13)
142. Jiang R, Qie X, Wu Z, Wang D, Liu M, Lu G, Liu D (2014) Characteristics of upward lightning from a 325-m-tall meteorology tower. *Atmos Res* 149:111–119
143. Lu W, Wang D, Zhang Y, Takagi N (2009) Two associated upward lightning flashes that produced opposite polarity electric field changes. *Geophys Res Lett* 36(5)
144. Mazur V, Ruhnke LH (2011) Physical processes during development of upward leaders from tall structures. *J Electrostat* 69(2):97–110
145. Wang D, Takagi N, Watanabe T, Sakurano H, Hashimoto M (2008) Observed characteristics of upward leaders that are initiated from a windmill and its lightning protection tower. *Geophys Res Lett* 35(2)
146. Brook M, Kitagawa N, Workman EJ (1962) Quantitative study of strokes and continuing currents in lightning discharges to ground. *J Geophys Res* 67(2):649–659
147. Schumann C, Hunt HG, Tasman J, Fensham H, Nixon KJ, Warner TA, Saba MM (2018a) High-speed video observation of lightning flashes over Johannesburg, South Africa 2017–2018. In: 2018 34th international conference on lightning protection (ICLP), pp 1–7
148. Paiva AR, Saba MMF, Naccarato KP, Schumann C, Jaques R, Ferro MAS, Warner TA (2014) Detection of upward lightning by lightning location systems, lightning protection (ICLP). In: International conference. Shanghai, pp 1824–1826

149. Diendorfer G, Pichler H, Schulz W (2014) EUCLID located strokes to the Gaisberg tower—accuracy of location and its assigned confidence ellipse. In: 2014 international lightning detection conference (ILDC)
150. Schwalt L, Pack S, Schulz W (2020) Ground truth data of atmospheric discharges in correlation with LLS detections. *Electr Power Syst Res* 180:106065
151. Chiumbu S (2012) Exploring mobile phone practices in social movements in South Africa—the Western Cape Anti-Eviction Campaign. *Afr Identities* 10(2):193–206
152. Southwood R (2009) *Less walk more talk: how Celtel and the mobile phone changed Africa*. Wiley, New York
153. Trengove E, Jandrell IR (2012) Leveraging a mobile culture for lightning awareness: the African context. In: Preprints of the 31st international conference on lightning protection. Vienna, pp 2–7
154. Wasserman H (2011) Mobile phones, popular media, and everyday African democracy: transmissions and transgressions. *Int J Media Cult* 9:146–158
155. Gire S (2017) The role of social media in the Arab Spring. <https://sites.stedwards.edu/pangaea/the-role-of-social-media-in-the-arab-spring/>. Accessed 8 Sept 2017
156. Lopez V (2017) On the frontline of Venezuela’s punishing protests. <https://www.theguardian.com/world/2017/may/25/venezuela-protests-riots-frontline-caracas-nicolas-maduro>. Accessed 30 Oct 2017
157. Wilson P (2014) Social media key for Venezuelan protesters. <https://www.usatoday.com/story/news/world/2014/02/19/venezuela-uprisingprotests/5606899/>. Accessed 8 Sept 2017
158. Gopalakrishnan V (2019) Early warning of lightning: lightning location network over India, RMLT(2019). Tripura University
159. Tushemereirwe R, Cooper MA, Tuhebwe D (2017) The most effective methods for delivering severe weather early warnings to fishermen on Lake Victoria. *PLOS Current Disasters*, 16, 22 Feb 2017
160. Kyazze F, Kristjanson P (2011) Summary of baseline household survey results: Rakai district, south central Uganda, CGIAR research program on climate change, and food security (CCAFS)
161. GSMA Development Fund (2010) *Women & mobile: a global opportunity—a study on the mobile phone gender gap in low-and middle-income countries*
162. Cooper MA, Holle RL (2019) *Reducing lightning injuries worldwide*. Springer Natural Hazards, Berlin